2014-12-01

# Characterization of Smoothness in Wrist Rotations

Layne Hancock Salmond
*Brigham Young University - Provo*

# Characterization of Smoothness in Wrist Rotations

Layne Hancock Salmond

A thesis submitted to the faculty of
Brigham Young University
in partial fulfillment of the requirements for the degree of

Master of Science

Steven K. Charles, Chair
Mark B. Colton
Brian D. Jensen

Department of Mechanical Engineering

Brigham Young University

December 2014

ABSTRACT

Characterization of Smoothness in Wrist Rotations

Layne Hancock Salmond
Department of Mechanical Engineering, BYU
Master of Science

Smoothness is a hallmark of healthy movement and has the potential to be used as a marker of recovery in rehabilitation settings. While much past research has focused on shoulder and elbow movements (reaching), little is known about movements of the wrist despite its importance in everyday life and its impairment in many neurological and biomechanical disorders. Our current lack of knowledge regarding wrist movement prevents us from improving current models, diagnosis, and treatment of wrist disorders. In particular, while movement smoothness is a well-known characteristic of reaching movements and may potentially be used to diagnose and monitor recovery from neurological impairments, little is known about the smoothness of wrist rotations. Therefore, because the smoothness of wrist rotations has not been characterized, it cannot be used as a marker for diagnosis and evaluation. This study examines the smoothness of wrist rotations in comparison to the known baseline of reaching movements. Subjects were asked to perform wrist and reaching movements under a variety of conditions, including different speed and direction. To measure movement smoothness, this study used an established metric of speed profile number of maxima and presents a novel method for characterizing smoothness by fitting a minimum-jerk trajectory to real movement data.

The results show that 1) wrist rotations are significantly less smooth than reaching movements ($p \leq 0.0016$), 2) smoothness decreases significantly as speed decreases ($p < 0.0001$), and 3) wrist movements exhibit a pattern of smoothness that varies significantly between targets and outbound/inbound movement directions ($p < 0.0001$). Potential causes for results 1 and 3 are presented and tested by simulation or reference to prior studies, because these findings were previously unknown. The decrease in smoothness with speed (result 2) has been found in prior studies of smoothness in reaching and finger movements. The reasoning behind the first result is explored by testing whether the difference in smoothness between wrist and reaching movements was due to differences in mechanical, muscular, neural, or protocol-related properties. The reasoning behind the third result is explored by testing whether the difference in wrist direction was due to anisotropy in musculoskeletal dynamics or anisotropy in movement duration. The simulations show that the wrist's bandwidth is greater than that of the arm, and that there is non-voluntary power in the bandwidth of the wrist that would be low-pass filtered in reaching movements, indicating that at least some of the difference in smoothness between wrist and reaching movements is due to differences in mechanical properties. Differences in muscular, neural, or protocol-related properties (signal-dependent noise, proprioceptive acuity, and the speed requirements of the task, respectively) do not appear to be the cause of the difference in smoothness between wrist and reaching movements. Differences in wrist smoothness between movement directions appears to be related to differences in movement duration between directions.

Keywords: movement, kinematics, smoothness, minimum jerk, motor control

ACKNOWLEDGEMENTS

I would like to give thanks to Matthew Marshall and Andrew Davidson for assisting me with programming and simulation testing. I would especially like to thank Dr. Steven K. Charles for mentoring me through this research and his confidence in me. I would also like to thank my wife, Breanne Salmond, for supporting me from the sidelines.

TABLE OF CONTENTS

LIST OF TABLES

LIST OF FIGURES

# 1 INTRODUCTION

Smoothness, or the lack of jerkiness, is a hallmark of healthy movement. Many studies have characterized the smoothness of brief eye and arm movements, and these studies found that these movement's speed profiles are generally unimodal and bell-shaped (Morasso, 1981; Atkeson and Hollerbach, 1985; Harris and Wolpert, 1998) (See Figure 1-1). Flash and Hogan (1985) found that via-point movements were well-approximated by assuming the movement maximized smoothness by minimizing jerkiness. The importance and potential reason for smooth movements is to minimize the deviation at the endpoint (Harris and Wolpert, 1998). However, some neurological signal variance (caused by signal-dependent noise) is introduced during a movement that prevents it from being perfectly smooth. The signal-dependent noise is the reason why smoother movements have less endpoint error. To have less endpoint error and smoother movements, movements reduce the signal-dependent noise by minimizing movement jerkiness.

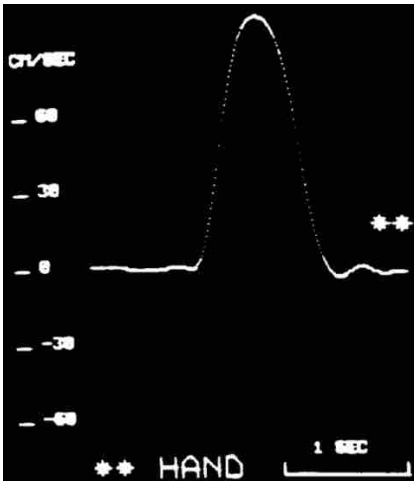


**Figure 1-1: Typical Speed Profile - Demonstrates stereotypical smooth movement (Morasso, 1981).**

Smoothness (or lack thereof) could be used as marker for disorders and rehabilitation. Patients with movement disorders (such as stroke) often exhibit jerky reaching movements with speed profiles containing multiple peaks (Rohrer et al., 2002). Remarkably, recovery from movement disorders has been shown to be accompanied by an increase in movement smoothness (Rohrer et al., 2002, 2004; Dipietro et al., 2009). Consequently, the smoothness of reaching movements may potentially be used to diagnose and monitor recovery from disorders which affect reaching movements. This approach is especially appealing when coupled with rehabilitation robotics since the robot could monitor changes in movement smoothness during therapy (Hogan et al., 2006).

While reaching movements have been extensively studied for these purposes, wrist rotations have not. There is no baseline of smoothness for wrist movements that could be used for movement disorders or diagnosis. Consequently, despite the development and implementation of robotic rehabilitation for the wrist (Krebs et al., 2007), analyzing wrist rotation smoothness is not currently useful to diagnose or monitor recovery from disorders affecting wrist rotations.

This research uncovers a novel method of quantifying smoothness, characterizes the smoothness of healthy wrist rotations, and compares those wrist rotations to a baseline of healthy reaching movements. This study found that wrist rotations are significantly less smooth than reaching movements, faster wrist rotations are smoother than slower wrist rotations, and wrist movement exhibits a pattern of smoothness that varies between targets and outbound/inbound movement directions. The increase in smoothness with speed has been seen for reaching and finger movements in prior studies (Brooks et al., 1973; Vallbo and Wessberg, 1993; Doeringer and Hogan, 1998), so this study focused on explaining the newly discovered phenomena. More

specifically, this study explores possible causes for differences in smoothness between joints and movement directions by simulating arm and wrist movements that we can compare to the actual data.

In this thesis, Chapter 2 explains the novel method of obtaining smoothness and shows the method in practice. Chapter 3 outlines the methodology of the experiment. Chapter 4 shows the results of analyzing the data of the experiment. Chapter 5 explains the simulations used to evaluate the findings and the results of the movement simulations. Chapter 6 discusses the causes underlying the major findings from the experiments and the limitations of the findings and experiment.

# 2 FITTING A MINIMUM-JERK TRAJECTORY TO REAL DATA

## 2.1 Introduction

Jerk (the time derivative of acceleration) is commonly used to describe movement smoothness (Hogan, 1984). When squared and integrated over the duration of a movement, jerk provides a quantitative (inversely related) measure of the smoothness of that movement, and the smoothest possible movement can be defined as the movement that minimizes $\int_0^d \dddot{x}^2 dt$, the integrated square jerk (ISJ) (Flash and Hogan, 1985). The minimum-jerk trajectory (MJT) of a movement that starts and ends at rest (zero velocity and acceleration) has a well-known equation that depends only on the time and position at the start and end (Flash and Hogan, 1985). However, it is difficult to compare a real (experimentally measured) movement to its equivalent MJT because the exact start and end times and positions of real movements are usually not well defined. Even discrete movements usually exhibit an extended period of low (but non-zero) velocity and acceleration before and after a movement, making estimation of the exact start and end times inaccurate. For this reason, the start and end of real movements are often defined through a threshold condition, such as when the speed exceeds a percentage (often 5% or 10%) of the peak speed. Because the equation for the MJT assumes different boundary conditions (zero speed and acceleration at the start and end) than the threshold condition, fitting a MJT to real movement data defined by a threshold condition results in an incorrect fit.

Here we present a novel method for correctly fitting a MJT to real movement data defined by a threshold condition. More specifically, we derive the time and position at the start and end of the MJT that satisfies the same threshold condition as the real movement (same position and same percentage of maximum speed). This method enables users to accurately fit (and therefore compare) a MJT to a real movement. This is useful in rehabilitation because it provides a limit on the amount of improvement that is possible. This method also allows comparisons between different types of movements (e.g., wrist and reaching movements) because they can be compared on the basis of how closely they resemble their respective MJTs.

## 2.2 Method

### 2.2.1 Problem Definition

*Given*: $\boldsymbol{x}(t) = [x_1(t),\ x_2(t),\ x_3(t)]^T$, a real movement trajectory through three-dimensional space, where $t$ and $T$ represent time and the transpose operator, respectively. This trajectory is defined over the time interval $t_1 \leq t \leq t_2$ and has the following boundary conditions:

$$\|\dot{\boldsymbol{x}}(t_1)\| = \alpha\|\dot{\boldsymbol{x}}\|_{max} \tag{2-1}$$

$$\|\dot{\boldsymbol{x}}(t_2)\| = \alpha\|\dot{\boldsymbol{x}}\|_{max} \tag{2-2}$$

where $\|\dot{\boldsymbol{x}}(t)\| = \sqrt{[\dot{x}_1(t)]^2 + [\dot{x}_2(t)]^2 + [\dot{x}_3(t)]^2}$ is the speed of the trajectory at time $t$, $\|\dot{\boldsymbol{x}}\|_{max}$ is the maximum speed between $t_1$ and $t_2$, and $\alpha$ is a proportional constant (often 5% or 10%). As explained in the introduction to this chapter, $\boldsymbol{x}(t)$ is often extracted (from a longer data set containing multiple movements) to represent a single movement, the boundary conditions serving to find $t_1$ and $t_2$.

*Find*: $\hat{\boldsymbol{x}}(t) = [\hat{x}_1(t),\ \hat{x}_2(t),\ \hat{x}_3(t)]$, the MJT that fits the real movement trajectory as described in the following conditions.

*Conditions*: $\hat{\boldsymbol{x}}(t)$ is said to fit $\boldsymbol{x}(t)$ if they share the same position and proportion of their respective peak speeds at $t_1$ and $t_2$ (illustrated for a one-dimensional trajectory in Figure 2-1):

$$\hat{\boldsymbol{x}}(t_1) = \boldsymbol{x}(t_1) \tag{2-3}$$

$$\hat{\boldsymbol{x}}(t_2) = \boldsymbol{x}(t_2) \tag{2-4}$$

$$\left\|\dot{\hat{\boldsymbol{x}}}(t_1)\right\| = \alpha\left\|\dot{\hat{\boldsymbol{x}}}(t)\right\|_{max} \tag{2-5}$$

$$\left\|\dot{\hat{\boldsymbol{x}}}(t_2)\right\| = \alpha\left\|\dot{\hat{\boldsymbol{x}}}(t)\right\|_{max} \tag{2-6}$$

Note that it is generally true that $\left\|\dot{\hat{\boldsymbol{x}}}(t_1)\right\| \neq \|\dot{\boldsymbol{x}}(t_1)\|$ and $\left\|\dot{\hat{\boldsymbol{x}}}(t_2)\right\| \neq \|\dot{\boldsymbol{x}}(t_2)\|$.

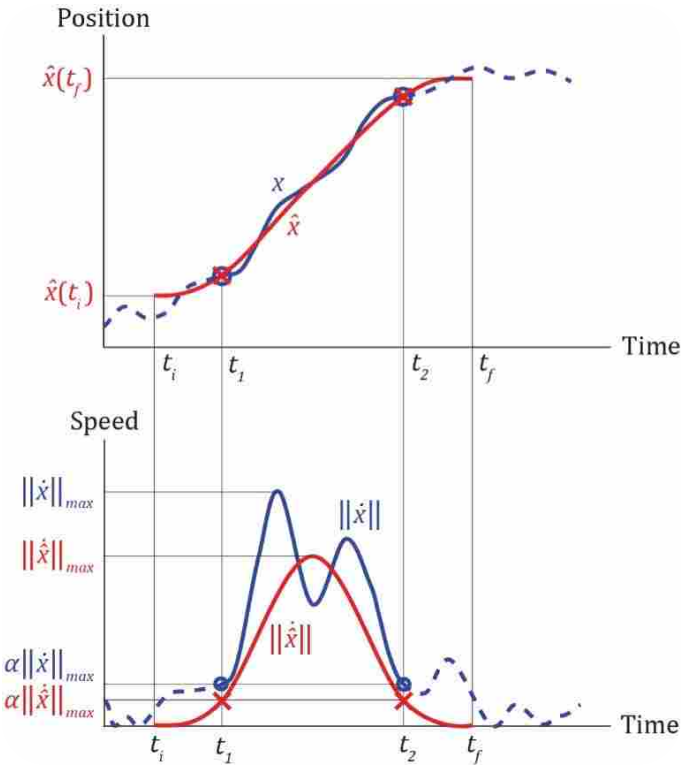


**Figure 2-1: Single Degree of Freedom with Terminology - Movement (blue) and MJT (red) for a fictitious movement in a single degree of freedom. The position and speed of the movement and corresponding MJT are shown in black and gray, respectively. The position and velocity at $t_1$ and $t_2$ (where the speed is a percentage of the maximum speed, the percentage being $100\alpha$) are indicated by circles (for the actual movement) or crosses (for the MJT). Note that the conditions 2-3 to 2-6 require that the position of the MJT match the position of the actual movement at $t_1$ and at $t_2$, and that the speed of the MJT be $\alpha$-times its maximum speed at $t_1$ and at $t_2$. The irrelevant portion of the movement (before $t_1$ and after $t_2$) is dashed.**

### 2.2.2 Solution

A MJT through three-dimensional space is given in Flash and Hogan (1985) as

$$\hat{\boldsymbol{x}}(t) = \hat{\boldsymbol{x}}(t_i) + \left[\hat{\boldsymbol{x}}(t_f) - \hat{\boldsymbol{x}}(t_i)\right]\left[10\left(\frac{t-t_i}{d}\right)^3 - 15\left(\frac{t-t_i}{d}\right)^4 + 6\left(\frac{t-t_i}{d}\right)^5\right] \quad (2\text{-}7)$$

where $\hat{\boldsymbol{x}}(t)$ is defined over the interval $t_i \le t \le t_f$ and $d$ is the movement duration defined as $d = t_f - t_i$.

Therefore, the task of finding $\hat{\boldsymbol{x}}(t)$ reduces to identifying $t_i$, $t_f$, $\hat{\boldsymbol{x}}(t_i)$, and $\hat{\boldsymbol{x}}(t_f)$. Times $t_i$ and $t_f$ can be found from conditions 2-5 and 2-6 as follows. First, the speed of the MJT is derived from velocity:

$$\dot{\hat{\boldsymbol{x}}}(t) = \frac{30[\hat{\boldsymbol{x}}(t_f) - \hat{\boldsymbol{x}}(t_i)]}{d}\left[\left(\frac{t-t_i}{d}\right)^2 - 2\left(\frac{t-t_i}{d}\right)^3 + \left(\frac{t-t_i}{d}\right)^4\right] \quad (2\text{-}8)$$

$$\left\|\dot{\hat{\boldsymbol{x}}}(t)\right\| = \frac{30\left\|\hat{\boldsymbol{x}}(t_f) - \hat{\boldsymbol{x}}(t_i)\right\|}{d}\left[\left(\frac{t-t_i}{d}\right)^2 - 2\left(\frac{t-t_i}{d}\right)^3 + \left(\frac{t-t_i}{d}\right)^4\right] \quad (2\text{-}9)$$

where

$$\left\|\hat{\boldsymbol{x}}(t_f) - \hat{\boldsymbol{x}}(t_i)\right\| = \sqrt{[\hat{x}_1(t_f) - \hat{x}_1(t_i)]^2 + [\hat{x}_2(t_f) - \hat{x}_2(t_i)]^2 + [\hat{x}_3(t_f) - \hat{x}_3(t_i)]^2} \quad (2\text{-}10)$$

The maximum speed can be found by setting the time derivative of speed to zero:

$$\frac{d}{dt}\left\|\dot{\hat{\boldsymbol{x}}}(t)\right\| = \frac{60\left\|\hat{\boldsymbol{x}}(t_f) - \hat{\boldsymbol{x}}(t_i)\right\|}{d^2}\left[\left(\frac{t-t_i}{d}\right) - 3\left(\frac{t-t_i}{d}\right)^2 + 2\left(\frac{t-t_i}{d}\right)^3\right] = 0 \quad (2\text{-}11)$$

Equation 2-11 is satisfied when $\left(\frac{t-t_i}{d}\right) = \frac{1}{2}$.

Evaluating equation 2-9 at this normalized time yields

$$\left\|\dot{\hat{\boldsymbol{x}}}(t)\right\|_{max} = \frac{15\left\|\hat{\boldsymbol{x}}(t_f) - \hat{\boldsymbol{x}}(t_i)\right\|}{8d} \quad (2\text{-}12)$$

Second, condition 2-5 requires that

$$\left\|\dot{\hat{\boldsymbol{x}}}(t_1)\right\| = \frac{30\left\|\hat{\boldsymbol{x}}(t_f) - \hat{\boldsymbol{x}}(t_i)\right\|}{d}\left[\left(\frac{t_1-t_i}{d}\right)^2 - 2\left(\frac{t_1-t_i}{d}\right)^3 + \left(\frac{t_1-t_i}{d}\right)^4\right] \quad (2\text{-}13)$$

be equal to

$$\alpha\left\|\dot{\hat{\boldsymbol{x}}}(t)\right\|_{max} = \alpha\frac{15\left\|\hat{\boldsymbol{x}}(t_f)-\hat{\boldsymbol{x}}(t_i)\right\|}{8d} \tag{2-14}$$

which, assuming that $\hat{\boldsymbol{x}}(t_f) \neq \hat{\boldsymbol{x}}(t_i)$, reduces to

$$\left(\frac{t_1-t_i}{d}\right)^4 - 2\left(\frac{t_1-t_i}{d}\right)^3 + \left(\frac{t_1-t_i}{d}\right)^2 - \frac{\alpha}{16} = 0 \tag{2-15}$$

Third, condition 2-6 likewise requires that

$$\left(\frac{t_2-t_i}{d}\right)^4 - 2\left(\frac{t_2-t_i}{d}\right)^3 + \left(\frac{t_2-t_i}{d}\right)^2 - \frac{\alpha}{16} = 0 \tag{2-16}$$

Substituting $u_1 = \frac{t_1-t_i}{d}$ and $u_2 = \frac{t_2-t_i}{d}$ into equations 2-15 and 2-16 yields

$$u_{1,2}{}^4 - 2u_{1,2}{}^3 + u_{1,2}{}^2 - \frac{\alpha}{16} = 0 \tag{2-17}$$

where $0 < u_1 < 1$, $0 < u_2 < 1$, and $u_2 > u_1$.

We solved equation 2-17 numerically for two common values of $\alpha$:

$$u_1 = 0.059434 \text{ for } \alpha = 0.05 \text{ and } u_1 = 0.086547 \text{ for } \alpha = 0.10 \tag{2-18}$$

$$u_2 = 0.94057\ \alpha = 0.05 \text{ and } u_2 = 0.91345 \text{ for } \alpha = 0.10 \tag{2-19}$$

Values for $t_i$, $d$, and $t_f$ can now be obtained from the definitions of $u_1$, $u_2$, and $d$, yielding

$$t_i = \frac{u_2t_1-u_1t_2}{u_2-u_1} \tag{2-20}$$

$$d = \frac{t_2-t_1}{u_2-u_1} \tag{2-21}$$

$$t_f = t_i + d \tag{2-22}$$

Solutions for $\hat{\boldsymbol{x}}(t_i)$ and $\hat{\boldsymbol{x}}(t_f)$ can be found from conditions 2-3 and 2-4, which require that

$$\hat{\boldsymbol{x}}(t_1) = \hat{\boldsymbol{x}}(t_i) + \left[\hat{\boldsymbol{x}}(t_f) - \hat{\boldsymbol{x}}(t_i)\right]\left[10\left(\frac{t_1-t_i}{d}\right)^3 - 15\left(\frac{t_1-t_i}{d}\right)^4 + 6\left(\frac{t_1-t_i}{d}\right)^5\right] = \boldsymbol{x}(t_1) \tag{2-23}$$

$$\hat{\boldsymbol{x}}(t_2) = \hat{\boldsymbol{x}}(t_i) + \left[\hat{\boldsymbol{x}}(t_f) - \hat{\boldsymbol{x}}(t_i)\right]\left[10\left(\frac{t_2-t_i}{d}\right)^3 - 15\left(\frac{t_2-t_i}{d}\right)^4 + 6\left(\frac{t_2-t_i}{d}\right)^5\right] = \boldsymbol{x}(t_2) \tag{2-24}$$

From the definitions of $u_1$ and $u_2$, $t_1 - t_i = u_1d$ and $t_2 - t_i = u_2d$, so equations 2-23 and 2-24 reduce to the following system of linear equations:

$$\hat{\boldsymbol{x}}(t_i)\,(1-v_1)+\hat{\boldsymbol{x}}(t_f)v_1=\boldsymbol{x}(t_1) \tag{2-25}$$

$$\hat{\boldsymbol{x}}(t_i)\,(1-v_2)+\hat{\boldsymbol{x}}(t_f)v_2=\boldsymbol{x}(t_2) \tag{2-26}$$

where

$$v_1=10{u_1}^3-15{u_1}^4+6{u_1}^5 \tag{2-27}$$

$$v_2=10{u_2}^3-15{u_2}^4+6{u_2}^5 \tag{2-28}$$

Solving this system yields

$$\hat{\boldsymbol{x}}(t_i)\ =\frac{v_2\boldsymbol{x}(t_1)-v_1\boldsymbol{x}(t_2)}{v_2-v_1} \tag{2-29}$$

$$\hat{\boldsymbol{x}}(t_f)=\frac{(1-v_1)\boldsymbol{x}(t_2)-(1-v_2)\boldsymbol{x}(t_1)}{v_2-v_1} \tag{2-30}$$

Substituting the values for $u_1$ and $u_2$ (from equations 2-18 and 2-19) into equations 2-27 and 2-28 yields $v_1$ and $v_2$, and substituting $v_1$ and $v_2$ into equations 2-29 and 2-30 yields values for values for $\hat{\boldsymbol{x}}(t_i)$ and $\hat{\boldsymbol{x}}(t_f)$. Finally, substituting $\hat{\boldsymbol{x}}(t_i)$ and $\hat{\boldsymbol{x}}(t_f)$ and the values for $t_i$ and $t_f$ (from equations 2-20 and 2-22) into equation 2-7 yields the desired MJT.

## 2.3 Examples

To show how this novel method applies to real data, we have used this method to fit MJTs to two real movements (a fast and a slow movement; Figure 2-2) and have evaluated how closely each movement resembles its MJT. More specifically, we have calculated for each movement the ratio of its ISJ to that of its minimum-jerk equivalent. The smoothest possibly trajectory will have a ratio of 1.

We applied our method to these two planar shoulder and elbow (reaching) movements (See Figure 2-2) and calculated the amount of jerk for each movement and for the corresponding MJTs using $\alpha$ = 10%. Because the ISJ changes with movement duration (since it is integrated

over the movement duration) and the two real movements had different durations, we used the non-dimensional ISJ (Hogan and Sternad, 2009) as opposed to the ISJ to provide a fair comparison between the real movements. So, in summary, we defined our 2 degree of freedom non-dimensional ISJ as $\frac{d^5}{\Delta x_1{}^2 + \Delta x_2{}^2}\int_0^d (\dddot{x}_1{}^2 + \dddot{x}_2{}^2)dt$. Finally, for each movement we calculated the ratio of its non-dimensional ISJ to the non-dimensional ISJ of its MJT (which is the same as the ratio of the ISJ values because the real movement and corresponding fit have the same amplitude and duration), also known throughout this thesis as Jerk Ratio.

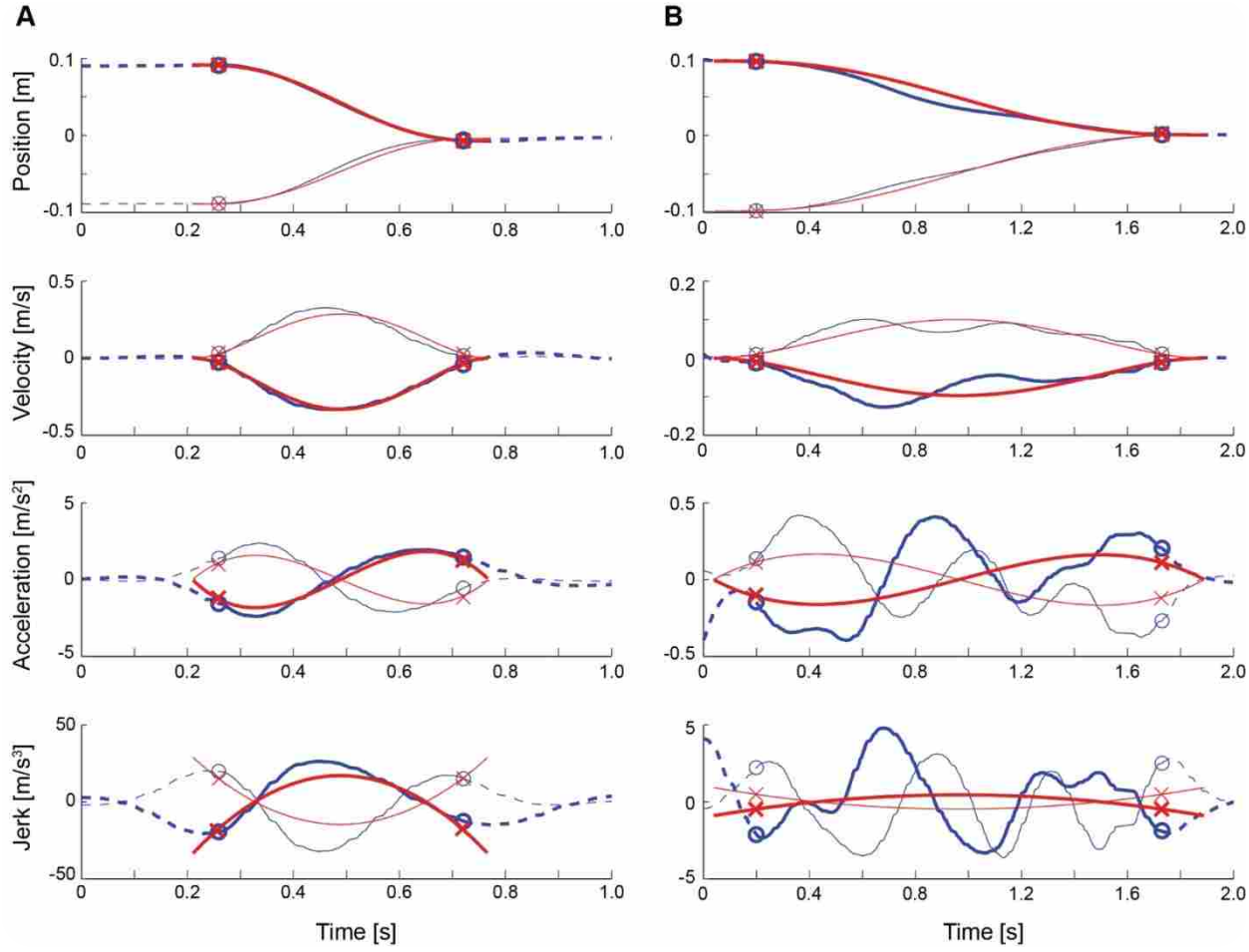


**Figure 2-2: Real Movements and Corresponding MJTs - These examples highlight a smooth movement (A) and a less smooth movement (B). The thick and thin lines represent the two degrees of freedom of the actual movement (blue) and the MJT (red). Times $t_1$ and $t_2$ (where the speed is $\alpha$ times the maximum speed) are indicated by circles (for the actual movement) or crosses (for the MJT). The irrelevant portion of the movement (before $t_1$ and after $t_2$) is dashed.**

For the first sample movement (See Figure 2-2A), the non-dimensional ISJ of the actual movement was 170, and the non-dimensional ISJ of the MJT was 140, resulting in an ISJ ratio of 1.2. For the second, slower sample movement (See Figure 2-2B), the non-dimensional ISJ of the actual movement was 2440, and the non-dimensional ISJ of the MJT was 140, resulting in an ISJ ratio of 17 (every MJT profile has the same non-dimensional ISJ for a given value of $\alpha$). As seen from these ratios and visually verified in Figure 2-2, the first sample movement is much smoother than the second sample movement.

## 2.4 Discussion of Novel Method of Fitting a Minimum-Jerk Trajectory to Real Data

Smoothness has the potential for use as a marker of the severity of a movement disorder, but it is currently not possible to compare a real (experimentally measured) movement to its equivalent maximally smooth (MJT) fit. To create a MJT requires the time and position at the start and end of the movement, but these parameters are usually not well defined for real movements. In practice, the "relevant portion" of real movements is often defined by a threshold condition, such as when the speed exceeds a percentage of peak speed (often 5% or 10%), which is not compatible with the standard equation for the MJT.

Here is presented a novel method for fitting a MJT to real data to fill this need. The MJT satisfies the same threshold condition as the real movement, accurately fitting the real movement while allowing the real movement to be specified in a standard form (defined by a threshold condition). Furthermore, by comparing the ISJ of the real movement to that of its MJT equivalent, this method provides a reference point, and the ratio of the two ISJ values gives a more meaningful measure than the ISJ—or even the non-dimensional ISJ (Hogan and Sternad, 2009)—of the real movement by itself.

We chose the constraints defined in equations 2-3 through 2-6 because (for simple destination movements) they are simple to identify and used commonly in practice. Alternatively, we could have matched the position, velocity, and acceleration of the actual movement and the MJT at $t_1$ and $t_2$, and used these boundary conditions to calculate new, movement-specific coefficients of the minimum-jerk polynomial (Hogan, 1984). In this approach, the velocity and acceleration of the actual movement at $t_1$ and $t_2$ would play a very important role (since they would dictate the velocity and acceleration of the MJT at those times), which may be problematic since the velocity and acceleration of real movements show significant moment-to-moment variability (this could lead, for example, to a situation where the MJT was constrained to start with negative acceleration). However, there may be situations in which these or other alternative constraints are better suited (e.g., movements that include waypoints or complex maneuvering). While we have presented the method for a 3-dimensional movement, it is easily applied to 1- or 2-dimensional movements, as was demonstrated above on two real, two-dimensional (planar reaching) movements.

When analyzing data, this method can be helpful for a number of applications. In motor control research, this method can be used to see how closely real movements approach their equivalent maximally smooth movements. Within the scope of rehabilitation, the reaching movements of patients with certain disorders (such as stroke) are irregular and less smooth, and their movement smoothness improves with recovery (Rohrer et al., 2002, 2004; Dipietro et al., 2009). This method can be used to evaluate a patient's progress by quantifying the approach of movements toward the smoothest possible movement, and is especially attractive in the era of rehabilitation robotics (Kwakkel et al., 2008) because the robot already measures kinematic variables and can easily calculate how they compare to their minimum-jerk equivalent. Also, this

method may eventually be used in conjunction with small mobile monitoring devices to track changes in smoothness for a variety of purposes, including evaluating patients' improvements in smoothness during activities of daily living after the end of formal rehabilitation; providing feedback for individuals learning a new skill (where greater smoothness often indicates greater skill); and monitoring the roughness of work-related movements (where less smoothness may be associated with impact and repetitive strain injuries).

# 3 EXPERIMENT METHODOLOGY

This research involved both experiment and simulation to characterize wrist rotations. First, the experiment methodology is outlined. Then, the simulation methodology is explained.

## 3.1 Subjects

Ten healthy human subjects (5 male, 5 female, age range 18–26, 23 ± 3 (mean ± StD) years of age) were recruited for data collection. None of the subjects had diagnosed neurological impairment or biomechanical injuries to the wrist. All subjects were right-handed and used their right upper limb for all trials (See Appendix A: Participant Data Sheet). IRB regulations were followed and each subject signed a consent form prior to the study.

## 3.2 Experimental Setup Common to Wrist and Reaching Experiments

Each experiment closely followed a written experimental protocol checklist to verify accuracy and consistency between tests (See Appendix B: Experiment Protocol). Subjects held a lightweight handle in their hand to which a motion sensor (trakSTAR) was rigidly attached. TrakSTAR is an electromagnetic motion sensing system (Angular Resolution: 0.021°, Linear Displacement Resolution: 0.0813mm, Linear Accuracy: 3.8mm RMS, Sampling Frequency ≈ 333Hz, Accuracy: 0.5° RMS) that consists of a transmitter and a number of sensors, and is

capable of tracking the six degrees of freedom of each sensor (3 positions and 3 orientations with time stamp).

There were two experimental setups to track movement. The first setup was used to study wrist rotation, while the second setup was used to study reaching motion.

## 3.3 Experimental Setup Unique to Wrist Experiment

Subjects were seated with the right forearm resting in a para-sagittal plane on the table in front of them.

The rotation of the forearm, pronation and supination (PS), was not important to this experiment. Therefore, PS was constrained during the experiment. To constrain the forearm, it was placed in an apparatus that clamped the distal forearm at three bony prominences (See Figure 3-1). This held the forearm in the para-sagittal plane and in neutral PS position, or midway between full pronation and full supination. The apparatus largely eliminated PS while interfering minimally with flexion-extension (FE) and radial-ulnar deviation (RUD) wrist rotations (See Figure 3-2).

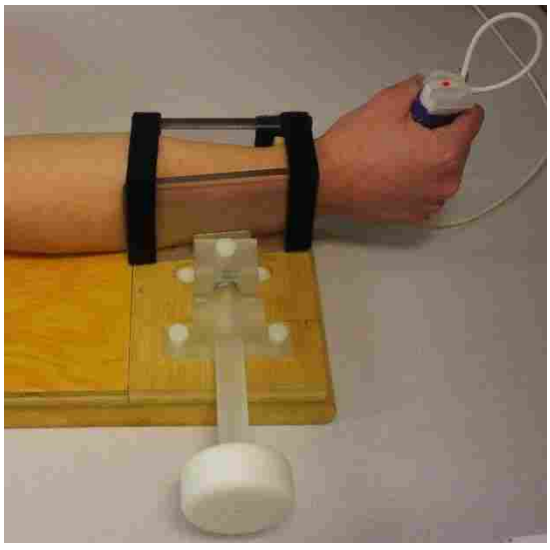

**Figure 3-1: Constraint Apparatus - Used to constrain pronation and supination of forearm.**

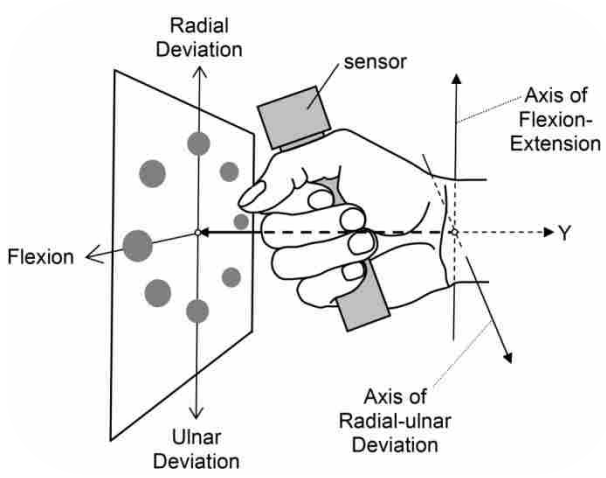


**Figure 3-2: Wrist Rotation Experiment - Terminology and setup. Figure modified from Charles and Hogan (2010).**

An adapted version of the International Society of Biomechanics recommendations was followed (Wu et al., 2005) to define neutral position. It was slightly adapted since ISB does not assume that subjects are holding a handle, so instead of aligning the 3rd metacarpal parallel with the long axis of the forearm for FE, we instead aligned the center of the handle with the long axis of the forearm. For RUD, the 3rd metacarpal still was aligned parallel to the long axis of the forearm.

## 3.4 Experimental Setup Unique to Reaching Experiment

Similar reaching experiments have been performed in the past, but this study evaluates reaching smoothness in similar conditions so that it can be accurately compared to the smoothness of wrist movements.

For the reaching portion, subjects were seated in a height adjustable chair, with a shoulder strap to minimize trunk movement by holding the subject's shoulder to the chair. Each subject's right forearm was placed in a sling to hold the arm and forearm approximately in the

horizontal plane, allowing only two degrees of freedom total at the shoulder and elbow (See Figure 3-3).

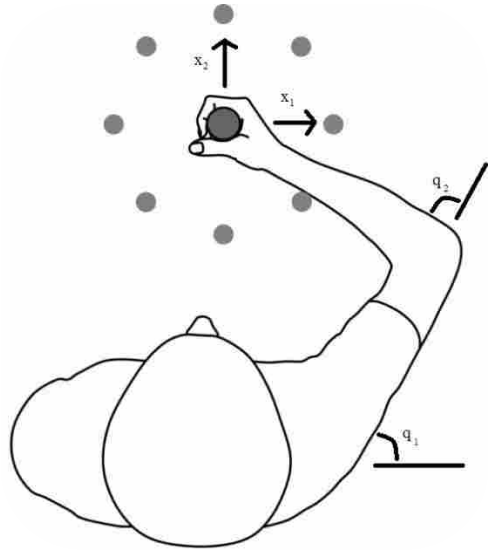


**Figure 3-3: Reaching Experiment - Setup and target location. Figure modified from Charles (2008).**

The right forearm was oriented mid-way between pronation and supination and the wrist was placed in a splint to prevent wrist rotation. The subject was asked to keep their hand shaped in a fist, but not to squeeze tightly. In their hand was placed the same motion sensor that was used in the wrist rotation portion. Neutral position was defined as 45° horizontal shoulder abduction ($q_1$) and 90° elbow flexion ($q_2$), where 0° was defined for both degrees of freedom when the arm was outstretched in the person's frontal plane.

## 3.5 Experimental Protocol for Wrist and Reaching Experiments

A computer monitor was placed approximately 80cm in front of the subjects, with 8 peripheral targets surrounding a central target (See Figure 3-4). Also shown was a cursor that corresponded to the orientation of the subject's wrist (for the wrist experiment) or the position of the subject's hand in the horizontal plane (for the reaching experiment). In neutral position, the

cursor was in the center target. Subjects were instructed to move from the center target to a peripheral target or from a peripheral target back to the center target in certain durations of time, as prompted by visual cues.

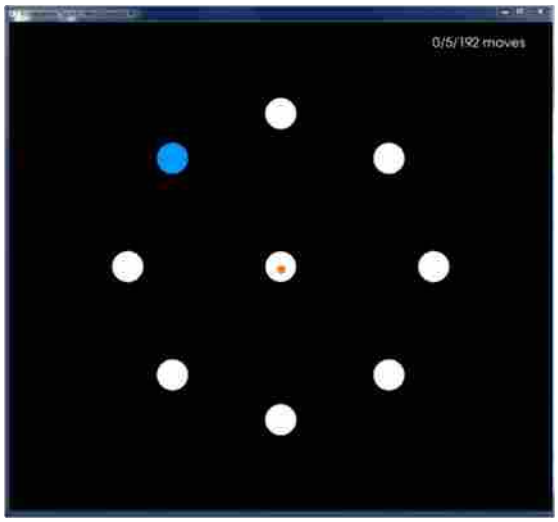


**Figure 3-4: Visual Display - Targets on monitor were numbered 1 through 8 counting clockwise from the top.**

For wrist experiments, subjects were asked to rotate their wrist in FE, RUD, or combinations. 15° of wrist rotation was required to move from a center target to one of the peripheral targets, or back. For reaching experiments, subjects were required to make shoulder and elbow (reaching) movements in different directions in the horizontal plane. 14cm of displacement of the hand was required to move from a center target to one of the peripheral targets, or back.

Each prompt was designed to elicit a discrete, separate movement by requiring that the subject come to a complete stop on the target and wait at least 0.6 seconds before the next target was displayed. Subjects were prompted to move to targets in random order for a total of 160 one-way moves per test (10 round-trip moves to each of the 8 targets).

To test if the smoothness of a movement changed with movement speed, the wrist and reaching tasks were each repeated with the same amplitude (15° or 14cm) but three different

movement durations (300 ± 75ms, 550 ± 100ms, and 900 ± 150ms) (which began when the cursor left the current target, and ended when the cursor entered the next target). These different durations produced 3 separate groups of fast, medium, and slow movements, and were chosen based on a study where subjects chose their own movement speed when instructed to make both wrist rotations and reaching movements "at a comfortable speed" and "as fast as possible" (Charles and Hogan, 2010).

Subjects had 32 practice moves at the beginning of each task. After every movement, the subject received text feedback on the monitor regarding the duration of the movement to help the subject remain within tolerance of the target time to travel (See Appendix C: Instructional PowerPoint). The tasks were completed in a random order between the six tasks (wrist vs. arm, three different speeds) with 3 minute breaks between tasks. Subjects were instructed in the beginning of the study to attempt to make "continuous and straight movements", but no instructions were given regarding movement smoothness.

### 3.6 Data Processing

Over the course of the experimentation, I recorded 10 subjects making a minimum of 10 roundtrip (2-way) movements to 8 targets at 3 different speeds with both the arm and wrist, for a total of over 9600 movements to process. Rest periods and the moves that had durations outside their respective ranges were removed for data processing. The output coordinates for the wrist were Euler angles in 2 rotational degrees of freedom, FE and RUD. Relatively small angular displacements (≤15° in each direction) have been justified as being projected in a Cartesian plane with little distortion (Charles and Hogan, 2010), so the cursor on the monitor projected the angles onto a plane. However, the Euler angles of FE and RUD used a linear approximation of ISJ so that the method was similar to the Cartesian methods used for reaching. Each move within

the duration range was defined as beginning and ending at 10% of the maximum of the Cartesian-space velocity magnitude of the entire movement. This approximation is a common assumption used on real data to isolate real movements, which do not have clear beginning and endings where the velocity is zero.

For filtering purposes, the data were resampled to have 333Hz sampling frequency. I analyzed the movement of the cursor in its 2 degree of freedom plane.

To get the speed, acceleration, and jerk data, the position data were numerically differentiated with the Matlab *diff* function. After each differentiation, the data was filtered by a $6^{th}$ order Butterworth filter at 15Hz cut-off frequency (more detail in Section 3.7). The beginning and end of each movement within the duration tolerance were then determined by taking the magnitude of the movement and finding the point of 10% of the speed maximum. The data were then ready to have the equivalent minimum-jerk trajectory applied to the movement and be analyzed for smoothness measures.

The smoothness of each movement was characterized using two measures: Jerk Ratio and the number of maxima (NumMax).

To compare the smoothness of each movement to a maximally smooth equivalent movement, I calculated the Jerk Ratio as the ratio of each movement's nondimensional integrated square jerk to the nondimensional integrated square jerk of the equivalent minimum-jerk trajectory (see Chapter 2). To calculate the minimum jerk of these movements, I created the novel method that is outlined in Chapter 2. The smoother the movement was, the closer the Jerk Ratio measure would be to 1.

I recorded the number of speed profile maxima peaks (or NumMax), similar to a number of past studies (Brooks et al., 1973; Hoffman and Strick, 1986; Fetters and Todd, 1987; Kahn et

al., 2001). NumMax is an indicator of how well the curve is bell-shaped or smooth. A move with only one maximum is considered fairly smooth, whereas a move with many maxima is considered as more jerky.

## 3.7 Filtering

**Figure 3-5: Magnitude Response of Filter – 6th order Butterworth filter at 15 Hz cut-off**

The data were filtered to remove the noise introduced by measuring instruments, and the noise was also amplified by differentiation. So, after each differentiation of the data, the data were filtered forward and backward (using Matlab's *filtfilt* function) using a 6th order Butterworth low-pass filter with a cut-off frequency at 15Hz to remove non-physiological noise (See Figure 3-5). The choice of order did not have a significant effect on the findings (See Section 4.2), and the cut-off frequency was chosen to be above the highest frequency of voluntary movements and above the frequency bandwidths of the arm and wrist. This was chosen because voluntary movement is generally below approximately 5Hz, and tapers off to almost nothing after 15Hz (See Figure 3-6).

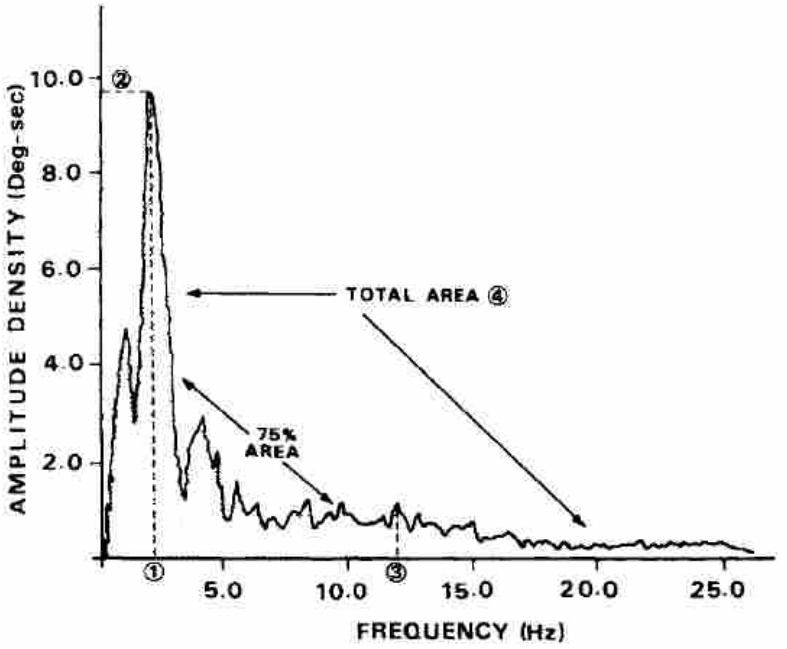


**Figure 3-6: Voluntary Movement Spectral Density – Content is low at high frequencies (Mann et al., 1989).**

Since the choice of filter properties affects the smoothness of the data that I am evaluating for smoothness, I did a study on the effect of filter properties on the smoothness measures and the major findings (See Appendix D: Effects of Filter Cut-Off Frequency and Order). I ran the data using 6$^{th}$ order Butterworth filters with cut-off frequencies 5Hz, 10Hz, 15Hz, 20Hz, and 25Hz, and also 2$^{nd}$ order filtering at 15Hz. The evaluation of this study can be found in Section 4.2.

## 3.8 Data Analysis

To compare the smoothness between factors (joint, speed, target, and direction), we performed statistical analyses on both Jerk Ratio and NumMax measures using three-way mixed-model ANOVA with subject as a random factor, and we used the Tukey-Kramer method for post-hoc analysis. For comparing reaching and wrist movements, each measure had joint (S/E vs. FE/RUD) and speed (300ms, 550ms, and 900ms) as fixed factors. For characterizing wrist

smoothness, the reaching experiment data were removed, and each measure had speed (300ms, 550ms, and 900ms), target (1-8), and direction (inbound vs. outbound) as fixed factors.

For purposes of the statistical analysis, Jerk Ratio was converted to $log_{10}(Jerk\ Ratio)$. This is due to the range of the Jerk Ratio measure varying greatly depending on the conditions. For plotting purposes, these values were converted back to their original value, but plotted on a logarithmic scale.

# 4 RESULTS

## 4.1 Experiment

The raw data of the experiment consisted of the timestamp, Cartesian-space position of the sensor for reaching movements or sensor angles projected to a plane for wrist rotations, indicators to specify between which targets the move was located, and whether the duration of the move was within the specified tolerance time.

Figure 4-1, Figure 4-2, and Figure 4-3 visually demonstrate the typical movement data that was used to analyze 300ms (fast), 550ms (medium), and 900ms (slow) movements, respectively. Each sample move displayed is an outbound movement to Target 1 performed by Subject 10, and represents the magnitude of both $x_1$ and $x_2$ for purposes of simplicity (which is a similar representation because movement in $x_2$ is small during this movement direction). Dark blue lines represent the real data before and after the start and stop of the movement. Cyan lines represent the real data that were evaluated. Magenta lines represent the equivalent minimum jerk trajectory for the movement. Green and red dots represent the moments the subject exits the previous target and enters the next target, respectively. Green and red circles represent the approximated beginning and end of the movement, which was determined by the 10% of the maximum speed criteria.

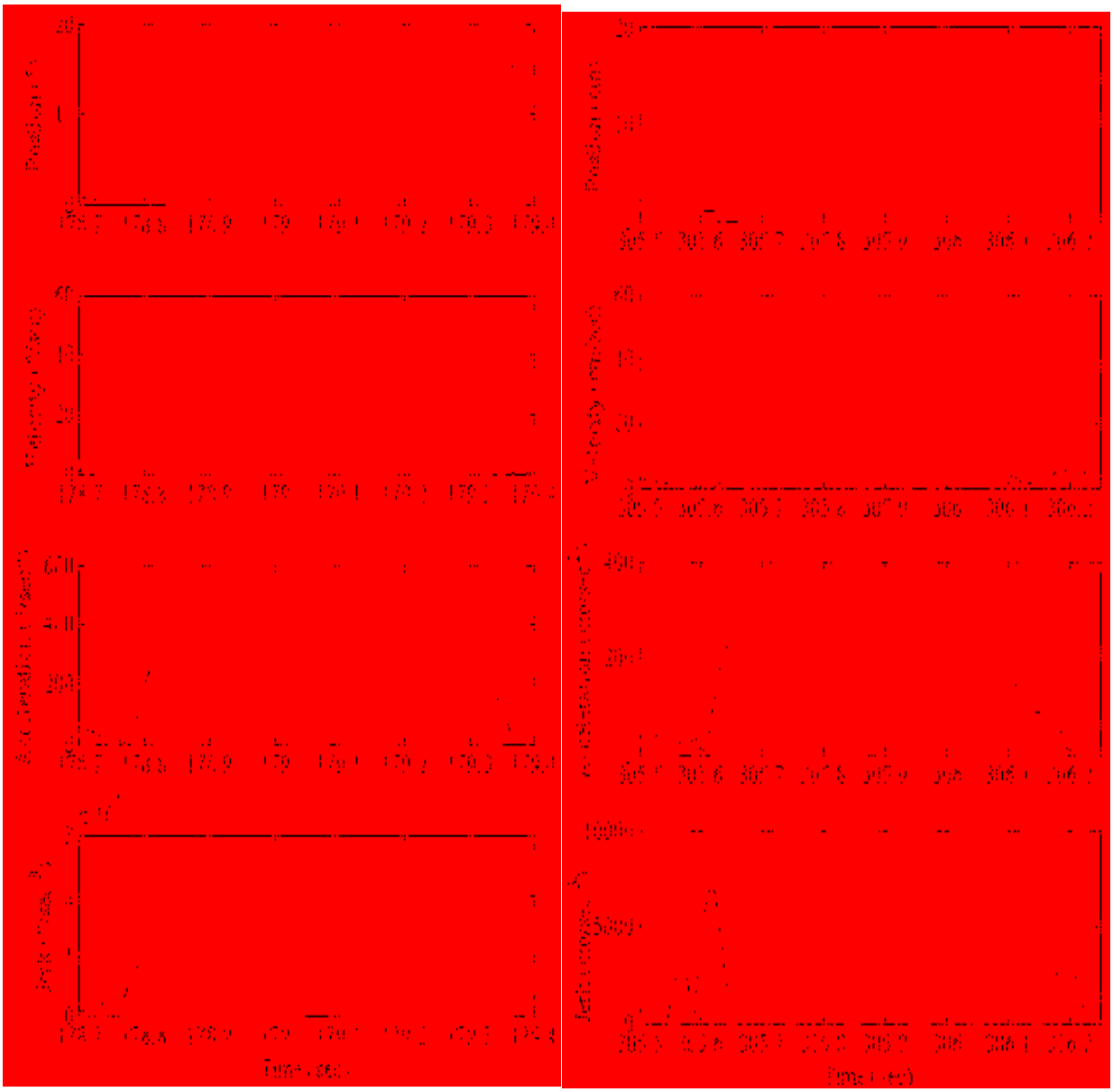

**Figure 4-1: Fast (300ms) Wrist and Reaching Data – Wrist on left, Reach on right.**

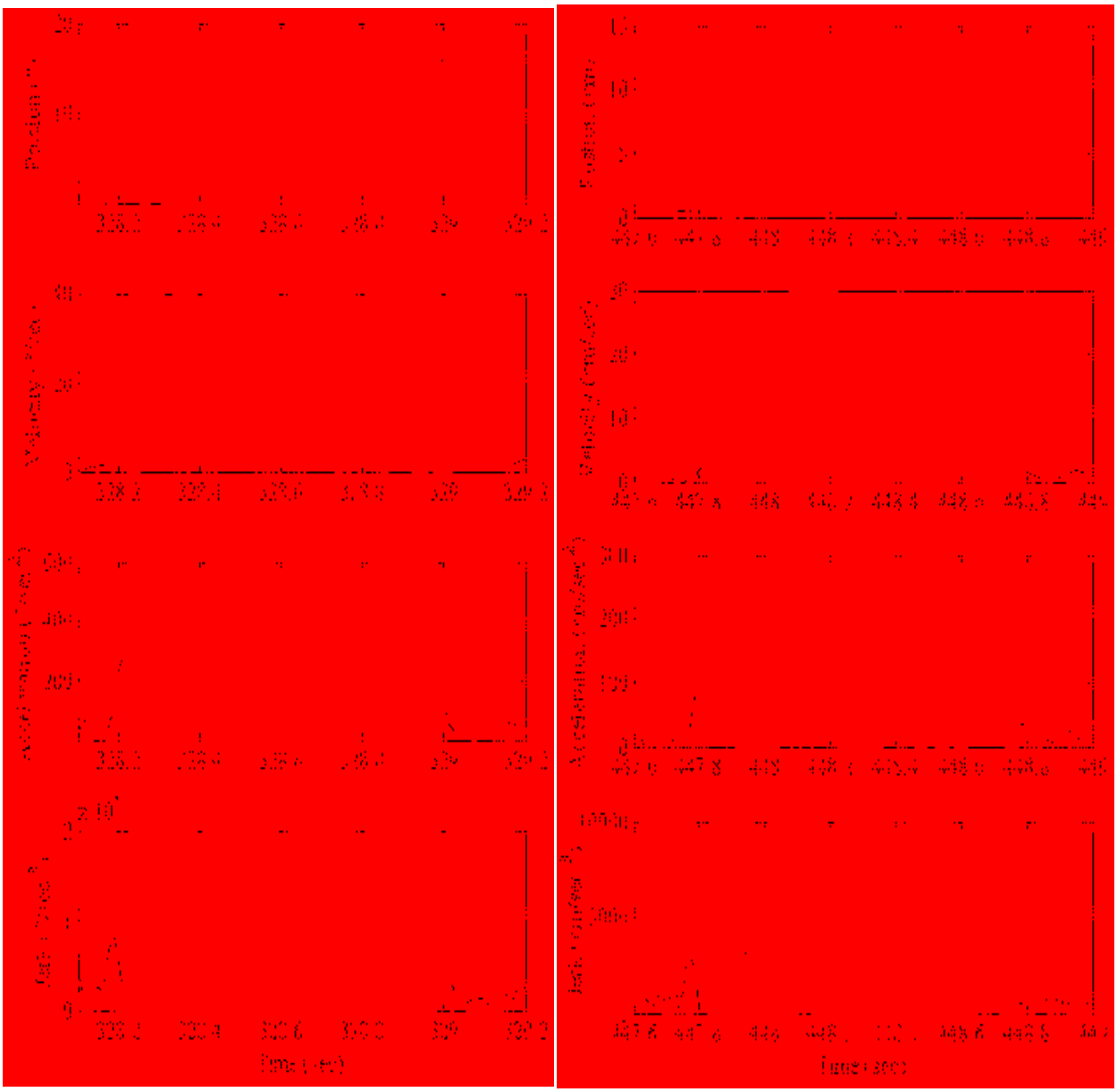

**Figure 4-2: Medium (550ms) Wrist and Reaching Data – Wrist on left, Reach on right.**

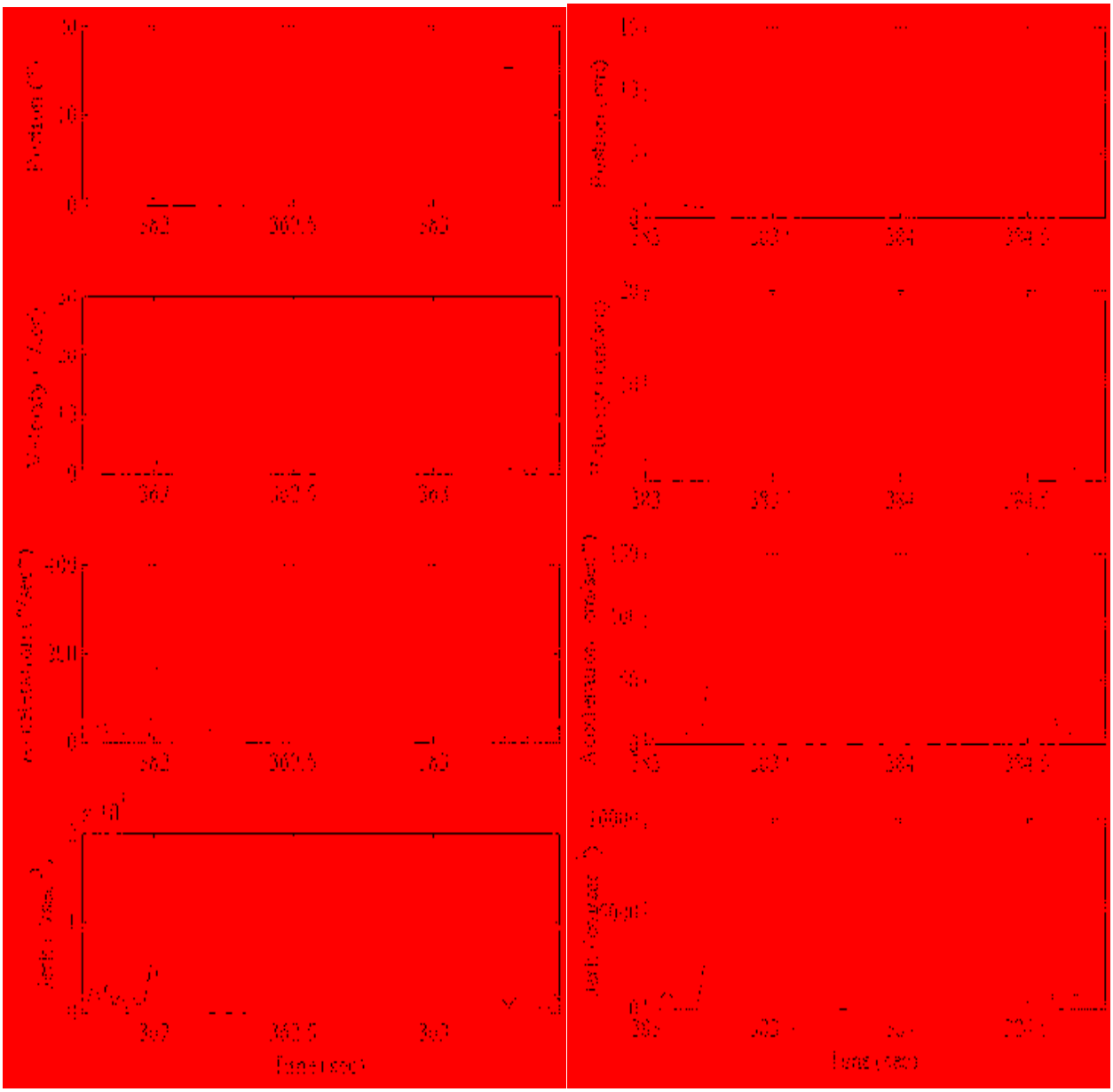

**Figure 4-3: Slow (900ms) Wrist and Reaching Data – Wrist on left, Reach on right.**

For Figure 4-4, smoothness measures (Jerk Ratio and NumMax) for joint and speed are on the top row of plots. Smoothness measures for wrist target and direction are on the bottom row of plots. For Table 4-1, each effect was significant ($p \leq 0.0065$).

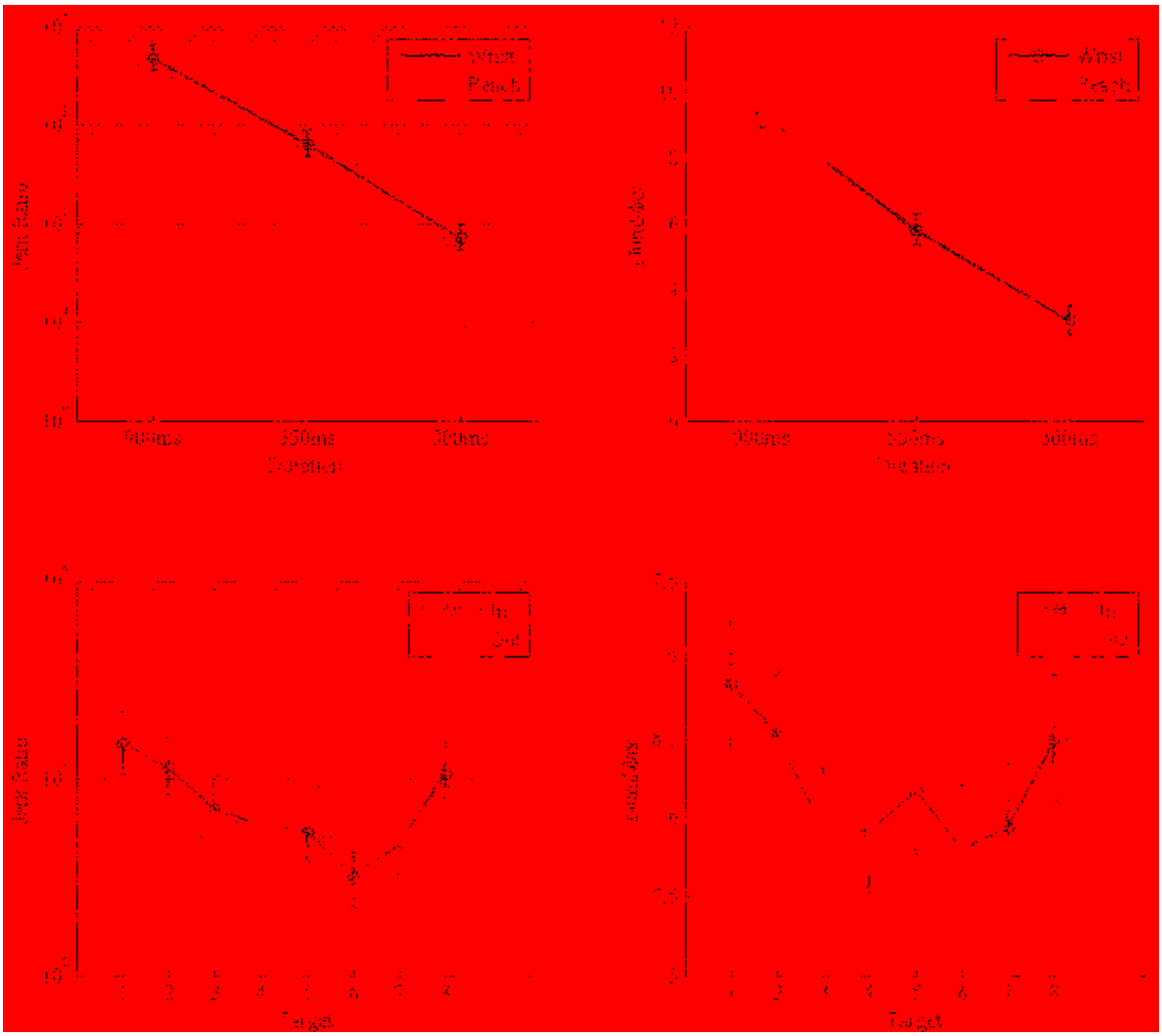

**Figure 4-4: Smoothness Measure Plot - Smoothness for joint and speed and for wrist target and direction.**

**Table 4-1: ANOVA p-Values - The p-values of each smoothness measure of critical factors and interactions.**

| Measure | Data | Effect | Num DF | Den DF | F Value | Pr > F |
|---|---|---|---|---|---|---|
| logJerkRatio | Reach/Wrist | Joint | 1 | 9 | 120.23 | <.0001 |
| logJerkRatio | Wrist only | Speed | 2 | 18 | 723 | <.0001 |
| logJerkRatio | Wrist only | Target | 7 | 63 | 5.75 | <.0001 |
| logJerkRatio | Wrist only | Direction | 1 | 9 | 30.61 | 0.0004 |
| logJerkRatio | Reach/Wrist | Joint*Speed | 2 | 18 | 6.75 | 0.0065 |
| logJerkRatio | Wrist only | Target*Direction | 7 | 63 | 32.98 | <.0001 |
| NumMax | Reach/Wrist | Joint | 1 | 9 | 19.76 | 0.0016 |
| NumMax | Wrist only | Speed | 2 | 18 | 505.69 | <.0001 |
| NumMax | Wrist only | Target | 7 | 63 | 6.64 | <.0001 |
| NumMax | Wrist only | Direction | 1 | 9 | 20.59 | 0.0014 |
| NumMax | Reach/Wrist | Joint*Speed | 2 | 18 | 27.59 | <.0001 |
| NumMax | Wrist only | Target*Direction | 7 | 63 | 6.89 | <.0001 |

### 4.1.1 Differences between Wrist Rotations to Reaching Movements

We found that wrist rotations are significantly less smooth than reaching movements (JR $p<0.0001$; NM $p=0.0016$; Table 4-1). The values of the smoothness measures were far greater (or less smooth) for wrist rotations than for reaching movements (See Figure 4-4).

### 4.1.2 Significance of Wrist Speed

We found that slower movements are less smooth than fast movements (JR & NM $p<0.0001$; Table 4-1). This is true for both wrist and reaching movements (See Figure 4-4). However, this trend was already known for reaching movements from previous studies (Doeringer and Hogan, 1998).

### 4.1.3 Significance of Wrist Direction

The difference in the smoothness between targets is statistically significant (JR & NM $p<0.0001$; Table 4-1) and the difference in the smoothness between directions is statistically significant (JR $p=0.004$; NM $p=0.0014$; Table 4-1). We also found wrist rotation smoothness varies significantly with the interaction between movement target and direction (inbound/outbound) (JR & NM $p<0.0001$; Table 4-1).

The pattern of smoothness shows interesting trends. The jerk ratio varies roughly sinusoidally with target direction, and the outbound and inbound patterns are 180° out of phase. The smoothest movements are inbound to Target 6, and outbound to Target 1, 2, and 8. The least smooth movements are inbound to Target 1, and outbound to Target 5, making an almost opposite pattern (See Figure 4-4 and Figure 4-5).

The patterns are similar for fast, medium, and slow movements, but the average pattern is almost exactly a scaled version of the pattern for slow movements because the jerk ratio for slow movements is so much larger than the jerk ratio for medium and fast movements.

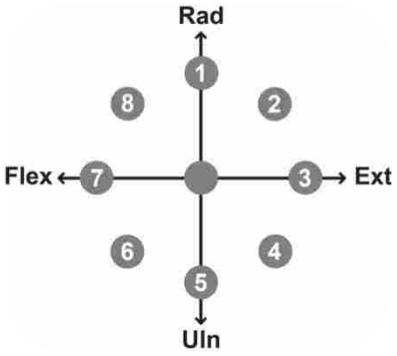


**Figure 4-5: Target Setup - Targets 1-8 labeled with each wrist rotation direction.**

## 4.2 Effect of Filtering on Jerk Ratio and NumMax

The low-pass filtering that I performed to reduce the noise from data collection clearly would affect the smoothness measure values, but it affects all the movements proportionally that were analyzed in the same way. Measures and statistics were re-calculated for five different filters: $6^{th}$ order Butterworth filters at 5Hz, 10Hz, 20Hz, and 25Hz cut-off frequencies; and a $2^{nd}$ order Butterworth filter at 15Hz cut-off frequency. The resulting plots and statistical tables are included in Appendix D: Effects of Filter Cut-Off Frequency and Order.

The values for Jerk Ratio naturally increase at higher cut-off frequencies, but the Jerk Ratio measure was consistent with the significance of major findings throughout the range of 5-25Hz cut-off frequencies. The number of maxima (NumMax), however, was not as robust against variations as the cut-off frequency increased. Depending on the cut-off frequency, the finding that wrist rotations were noisier than reaching wasn't always true, and the pattern in smoothness between targets was less consistent. The breakdown of NumMax is mostly due to the

higher frequency of peaks that are more apparent. For example, a slow wrist rotation is more likely to contain large variation in the speed profile, resulting in a number of large peaks with a few smaller peaks. NumMax does not account for the steepness of the slope on the sides of the peak, so each peak is counted the same. As another example, a slow reaching movement looks much more like a large minimum-jerk trajectory due to its smoother nature. However, the smaller higher frequency peaks are along the top of fairly horizontal speed plateaus. This allows these small peaks that are from high frequency noise to become more prevalent, and are counted the same as the fewer number of large peaks. This inflates the NumMax measure to inaccurately represent the smoothness with higher cut-off frequency filters.

Both measures show consistent results at most cut-off frequencies and are valuable for measuring smoothness and finding trends. However, the effect of filter cut-off frequency on Jerk Ratio is more robust than NumMax. Changing the properties of the filter affects the measure values, but does not affect the major findings and p-values for Jerk Ratio. However, changing these properties does drastically affect the NumMax values at higher cut-off frequencies. For cut-off frequencies below 20Hz, wrist movements are less smooth than reaching (Jerk Ratio and NumMax at $p<0.0001$). However, for cut-off frequencies at or above 20Hz, the NumMax measure broke down to say that reaching is less smooth than wrist movements, with p-values varying from $p<0.0001$ to $p=0.0011$, and Jerk Ratio measure was less significant, but still had wrist movements show as less smooth than reaching ($p\leq0.0034$). The pattern that smoothness increases with movement speed was not dependent on the cut-off frequency of the filter, with Jerk Ratio at $p<0.0001$ and NumMax at $p<0.0001$. The movement direction's pattern is consistent with Jerk Ratio, but varies a lot with the NumMax measure.

The only significant changes in p-values of the main effect of Target and the main effect of Direction are at the extreme high and low cut-off frequencies. Target main effect and Direction main effect are significant at 10-25 Hz with Jerk Ratio ($p \leq 0.0048$) because this shows there is a difference in low-pass filtering in the wrist, but this isn't as evident at the Target 5Hz cut-off frequency ($p=0.7637$). Also, the difference in the NumMax measure stays fairly significant at middle range cut-off frequencies ($p \leq 0.0728$), but is less significant at 5Hz and 25Hz ($p \geq 0.1831$). The NumMax measures are closer at higher and lower cut-off frequencies because the frequency content that causes the differences between smoothness are less drastic when the mid-frequency content is removed.

The order of the filter affects how sharp the roll-off is. Decreasing the order from 6 to 2, only two of the 12 p-values changed from significant to non-significant; one was an interaction, and the other concerned NumMax (which we know to be less robust than Jerk Ratio). Because the measures were not dependent on the order of the filter, I chose the $6^{th}$ order cut-off frequency to have a sharper roll-off.

# 5 SIMULATION AND COMPARISON

This study presents a number of potential causes underlying our findings and tests these hypotheses through simulation and a review of past studies. To determine the root cause of the major findings, I developed models to simulate some of the possible explanations for movement smoothness (or lack thereof).

To help the reader understand the choice of simulation methods, below presents a preview of the major findings (a detailed description of the findings can be found in Chapter 4):

1. Wrist rotations are significantly less smooth than reaching movements.
2. Slow wrist rotations are significantly less smooth than fast wrist rotations.
3. Wrist rotations in different directions exhibit significantly different smoothness.

The following hypothesis sections are labeled by the first number representing the finding which it addresses, and the second number representing the unique identifier of the hypothesis. The hypotheses and tests of the underlying causes are briefly organized in Table 5-1.

For major finding 2, the causes underlying the finding were not in the scope of this thesis, and can be future work. This finding was not particularly novel because it has been previously observed in movements, such as reaching (Doeringer and Hogan, 1998). Therefore, there are no hypotheses for finding 2 listed in this thesis.

**Table 5-1: Hypotheses and Tests – Hypotheses of underlying causes of the major findings, and the tests of how each hypothesis is explored.**

| | | | |
|---|---|---|---|
| 1 | Mechanical: The low-pass filtering properties of the wrist do not filter neuromuscular noise as well as those of the arm. | Using equations of motion for reaching and wrist movements, determine frequency response plots and bandwidths, then compare with the wrist and arm's frequency responses. | TRUE |
| 2 | Muscular: Distal muscles are noisier than proximal muscles | Using known coefficients of variation (SD/Mean) for proximal and distal muscles, create a model of the passive dynamics of the wrist and compare the smoothness that results from each type of movement | FALSE |
| 3 | Neural: Distal joints have less sensitive proprioception than proximal joints. | Literature search or grounded perception of each joint | FALSE |
| 4 | Protocol related: The study compared movements of the same duration, but the angular speeds are not equivalent | Compare wrist and reaching movements of similar angular velocities instead of duration and check whether difference in smoothness between joints persists | FALSE |
| 5A | The anisotropy in the skeletal dynamics of the wrist creates anisotropic torque fields creating asymmetry in stable/unstable zones | Using the model from hypothesis 1-2, compare variation of the wrist by modeling the smoothness of each direction | FALSE |
| 5B | Still movements observed in wrist speed profiles can be represented by using step torque input instead of minimum-jerk trajectory | Use the model from hypothesis 5-1A, except use a step torque input to model the movement. Compare how this change affects smoothness per each direction. | FALSE |
| 5C | Lower damping ratios have been found in other studies for the wrist. | Use the model from hypothesis 5-1B, except replace the damping and stiffness matrices with those from Hajian et al. (2) (3). | FALSE |
| 6 | Slightly longer movement durations are correlated with less smooth movement. | Plot each direction with the respective mean durations and compare the pattern found of direction and smoothness to find correlations. | TRUE |

## 5.1 Hypothesis 1-1: Mechanical Cause

Wrist low-pass filtering properties filter less than the shoulder/elbow low pass filtering. Movement smoothness is due to low-pass filtering of intrinsic muscle properties (Krylow and Rymer, 1997). Therefore, the low-pass filtering properties of the wrist do not filter the neuromuscular noise as well as those of the arm.

To observe if this was the cause, I needed to find the power spectrum of the data and compare that to the parameters' bode plots. If the bandwidth is higher for the wrist, and the power spectrum shows the presence of a low-pass filter, then this hypothesis is true.

### 5.1.1 Test for 1-1 Hypothesis

Linearized equations of motion for the arm and the wrist were used to simulate frequency response of the passive systems (i.e., in the absence of muscle activity). For the wrist's equation of motion, I used the linear equation from Charles and Hogan (2011), which states $I\ddot{\boldsymbol{q}} + D\dot{\boldsymbol{q}} +$

$K\boldsymbol{q} = \boldsymbol{\tau}$, where $\boldsymbol{q} = \begin{bmatrix} q_1 \\ q_2 \end{bmatrix}$ where $q_1$ is the angle for flexion-extension (positive in flexion) and $q_2$ is the angle for radial-ulnar deviation (positive in ulnar deviation). For the arm's equation of motion, I started with the nonlinear equation from Burdet et al. (2013), which states $H\ddot{\boldsymbol{q}} + C\dot{\boldsymbol{q}} = \boldsymbol{\tau}$, where $\boldsymbol{q} = \begin{bmatrix} q_1 \\ q_2 \end{bmatrix}$ where $q_1$ is the angle for the shoulder (positive in horizontal adduction) and $q_2$ is the angle for the elbow (positive in flexion), and $H$ is the inertial terms and $C$ is the Coriolis terms. I then expanded the equation to include active damping and stiffness, and then removed the nonlinear terms, which resulted in $I\ddot{\boldsymbol{q}} + D\dot{\boldsymbol{q}} + K\boldsymbol{q} = \boldsymbol{\tau}$, where $I$ is inertia, $D$ is damping, and $K$ is inertia. Using these formulas, I determined the bandwidth of the linearized equation of motion by solving for each joint's transfer functions and using the Matlab *bandwidth* and *bode* functions.

The wrist parameters were taken from Halaki et al. (2006), with some parameters scaled by Charles and Hogan (2012) (specifically the 2A dataset) and the reaching parameters were taken from Tee et al. (2004) and Burdet et al. (2013).

Then, I compared the bandwidth and the frequency response of actual data. This was obtained by taking one task's speed data (300ms Wrist, for example), truncating each subjects task to the shortest length of data of the subjects, and performing the power spectral density estimate via Welch's method (*pwelch* function in Matlab with scaled estimates of the power spectral density by the noise bandwidth of the window) on the data set. All 10 subjects were then averaged to represent the power spectrum of the task. This was repeated for each of the 6 tasks.

Then, I compared the bandwidth and the frequency response of minimum-jerk trajectory. This was obtained similarly to the method used with the actual data, but instead the data used were created using the durations of each correct movement to form minimum-jerk trajectories with 0.6sec resting time (speed set at 0) between each move.

By comparing the power spectrum of real wrist and reaching data to the ideal minimum-jerk trajectory and the bandwidth of the bode plot, I can determine if the jerkiness present in the wrist is a higher frequency signal that would be filtered out in the arm due to the mechanical properties that decreases the bandwidth of the low-pass filter.

### 5.1.2 Results of 1-1 Hypothesis

The power spectrum plots (See Figure 5-1) showed that the wrist exhibits noise in higher frequencies, especially around 7-10Hz that is not exhibited in reaching movements. The wrist high frequency noise tapers significantly after 10Hz, which is well before the influence of the filter applied on the data (15Hz cut-off frequency).

The arm does not exhibit the same unexpected high frequency noise. The arm's noise tapers significantly after 4Hz, which is well before the influence of the filter applied on the data (15Hz cut-off frequency). This is consistent with literature that finds the arm's filtering properties have a cut-off frequency of 2-3Hz (Burdet et al., 2013). The results support the hypothesis that low-pass filtering properties of the wrist do not filter neuromuscular noise as well as those of the arm.

The minimum jerk trajectory plot also showed interesting results. Reaching movements follow closely to the ideal simulated min jerk movements, which show that the trend observed is required for the movement the subject performed. This supports the hypothesis because noise would be filtered out after 3Hz. Wrist movements followed the ideal simulated min jerk movements between 0-3Hz, but shows significantly more noise until about 10Hz. There is also a spike of noise between about 7-10Hz. This supports the hypothesis because noise of the wrist isn't filtered until 10-12Hz.

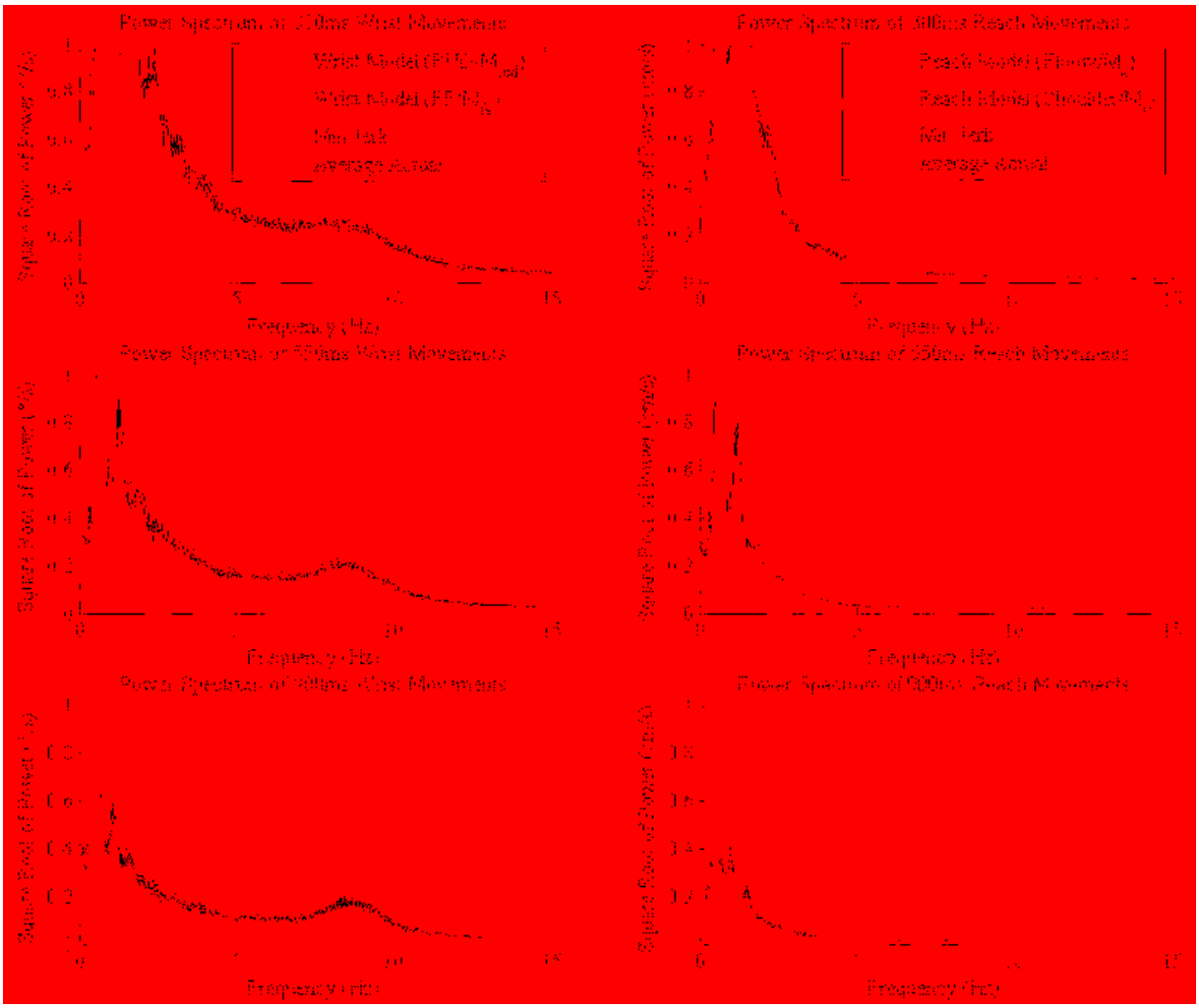

**Figure 5-1: Power Spectrum of Wrist and Arm - Power spectrum of bandwidth models of each joint, and the correlating minimum jerk model and average real data. The basic power spectrum bandwidth models are scaled, and do not correlate with the y-axis.**

The bandwidth of the arm is smaller than the bandwidth of the wrist. Therefore, if the inputs to the arm and wrist have noise with frequency in the difference band (3-5Hz to 10-12Hz), this noise will appear in wrist movements, but not in reaching movements. We do see power in the difference band for the wrist that is not required by the task (represented by the min-jerk power), so the wrist has noise. However, since we do not see a difference of power in the difference band between the output power and that required by the task (min-jerk), it is unclear whether there is noise being filtered out, or if the arm does not have the noise that the wrist does

have. It may be that not only is the wrist less good at low-pass filtering, but that it also has more input noise to low-pass filter.

The power spectrum of the data was comparable to that of the parameters' bode plots. The bandwidth was higher for the wrist, and the power spectrum showed the presence of a low-pass filter, so the hypothesis was true.

## 5.2 Hypothesis 1-2: Muscular Cause

The smaller, distal muscles that are present in the wrist are noisier than the larger, proximal muscles present in the arm. Noise in the output of the motor system appears to be signal-dependent (i.e. increases with muscle activity and, therefore, muscle force and joint torque). Prior studies have found that distal muscles have more variability than proximal muscles when producing the same amount of force (de C. Hamilton et al., 2004), but that this does not necessarily mean that distal muscles have more variability during movement since distal movements may require less force.

To observe if this was the cause, I needed to modify theoretical intended movement to include the noise mentioned above. If adding the noise made theoretical movements comparable to the results of the actual data, then this hypothesis is true.

### 5.2.1 Test for 1-2 Hypothesis

Using the known coefficients of variation for these muscles (de C. Hamilton et al., 2004), I created a model of movement dynamics that included the noise proportional to the feed forward torque, and computed the smoothness resulting from each type of movement. The coefficient of variation was 0.013 for the wrist and 0.005 for the arm. To simulate this noise, these coefficients

were multiplied by a normally distributed random signal that was scaled by the torque of the movement.

The model created a minimum jerk movement in Cartesian space ($\boldsymbol{x} = \begin{bmatrix} x_1 \\ x_2 \end{bmatrix}$), converted it to joint space ($\boldsymbol{q} = \begin{bmatrix} q_1 \\ q_2 \end{bmatrix}$ where $q_1$ is shoulder for reaching, and flexion for wrist), used inverse dynamics to solve for torque, added the noise, then used forward dynamics to have a noisier joint space movement, then converted it back to Cartesian space to solve for Jerk Ratio and NumMax just as the measures were solved for on the real data. This way, the effect of muscular signal variation can be observed on an ideal minimum-jerk trajectory, and we can evaluate how closely the resulting signal compares to actual movement data.

The transformation from wrist joint-space to task-space is $\begin{bmatrix} x_1 \\ x_2 \end{bmatrix} = \begin{bmatrix} -\sin(q_1)\cos(q_2) \\ -\sin(q_2) \end{bmatrix}$. The transformation from shoulder ($q_1$) and elbow ($q_2$) joint-space to task-space is $\begin{bmatrix} x_1 \\ x_2 \end{bmatrix} = \begin{bmatrix} L_1\cos(q_1) + L_2\cos(q_1 + q_2) \\ L_1\sin(q_1) + L_2\sin(q_1 + q_2) \end{bmatrix}$, where $L_1$ is the length of the upper arm and $L_2$ is the length of the forearm. These transformations are modified to also transform from task-space to joint-space.

The model of the control diagram (from desired joint space to simulated joint space) is explained in the following diagrams and equations, which show the theoretical model (See Figure 5-2), then the equivalent model for application into Matlab (See Figure 5-3):

The inverse dynamics for reaching feed forward torque is $H\ddot{\boldsymbol{q}}_u + C\dot{\boldsymbol{q}}_u = \boldsymbol{\tau}_{FF}$. The wrist feed forward torque is $I\ddot{\boldsymbol{q}}_u + D_p\dot{\boldsymbol{q}}_u + K_p\boldsymbol{q}_u = \boldsymbol{\tau}_{FF}$. The feedback torque for both reaching and wrist is $D_a\dot{\boldsymbol{e}} + K_a\boldsymbol{e} = \boldsymbol{\tau}_{FB}$. The torque noise that was proportional to the feed forward torque is added to both the feed forward torque and the feedback torque to simulate movement. The

forward dynamics then calculated the final position of the movement. The forward dynamics is $H\ddot{\boldsymbol{q}} + C\dot{\boldsymbol{q}} = \boldsymbol{\tau}_C$ for reaching, and $I\ddot{\boldsymbol{q}} + D_p\dot{\boldsymbol{q}} + K_p\boldsymbol{q} = \boldsymbol{\tau}_C$ for wrist.

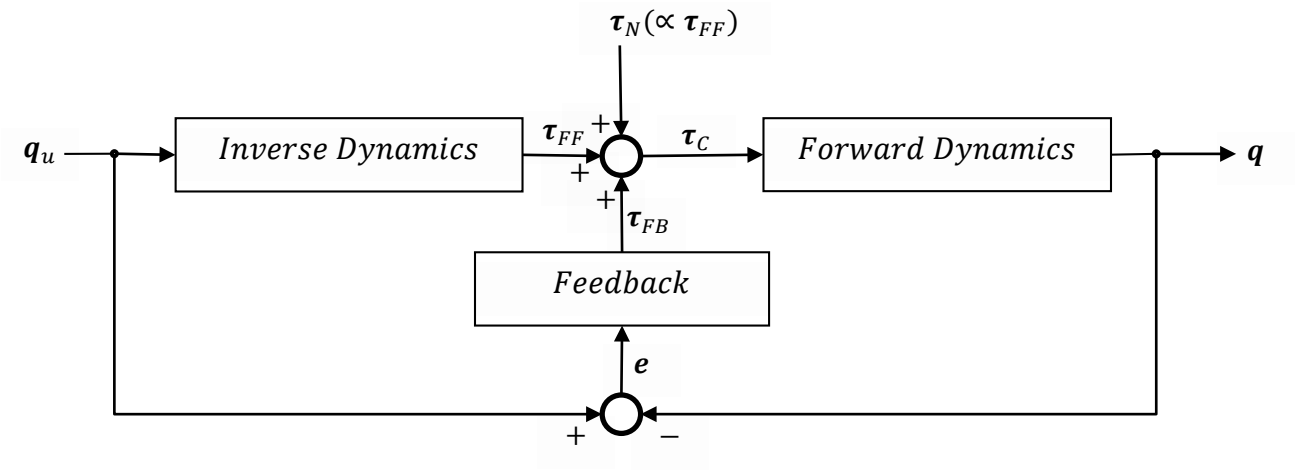


**Figure 5-2: Theoretical Control Diagram - Path from desired joint space to simulated joint space with forward dynamics, feedback, and inverse dynamics. Modified diagram courtesy of Dr. Charles.**

However, in order for this continuous system to be implemented in Matlab and have feedback of the actual movement, this had to be simplified. Below are the equations (5-1 to 5-7) for converting reaching, and the wrist follows a similar pattern.

$$H\ddot{\boldsymbol{q}} + C\dot{\boldsymbol{q}} = \boldsymbol{\tau}_C \tag{5-1}$$

$$H\ddot{\boldsymbol{q}} + C\dot{\boldsymbol{q}} = \boldsymbol{\tau}_{FF} + \boldsymbol{\tau}_N + \boldsymbol{\tau}_{FB} \tag{5-2}$$

$$H\ddot{\boldsymbol{q}} + C\dot{\boldsymbol{q}} = \boldsymbol{\tau}_{FF} + \boldsymbol{\tau}_N + D\dot{\boldsymbol{e}} + K\boldsymbol{e} \tag{5-3}$$

$$H\ddot{\boldsymbol{q}} + C\dot{\boldsymbol{q}} = \boldsymbol{\tau}_{FF} + \boldsymbol{\tau}_N + D(\dot{\boldsymbol{q}}_u - \dot{\boldsymbol{q}}) + K(\boldsymbol{q}_u - \boldsymbol{q}) \tag{5-4}$$

$$H\ddot{\boldsymbol{q}} + C\dot{\boldsymbol{q}} + D\dot{\boldsymbol{q}} + K\boldsymbol{q} = \boldsymbol{\tau}_{FF} + \boldsymbol{\tau}_N + D\dot{\boldsymbol{q}}_u + K\boldsymbol{q}_u \tag{5-5}$$

$$H\ddot{\boldsymbol{q}} + C\dot{\boldsymbol{q}} + D\dot{\boldsymbol{q}} + K\boldsymbol{q} = \boldsymbol{\tau}_{FF} + \boldsymbol{\tau}_N + \boldsymbol{\tau}_{FB,part} \tag{5-6}$$

$$H\ddot{\boldsymbol{q}} + C\dot{\boldsymbol{q}} + D\dot{\boldsymbol{q}} + K\boldsymbol{q} = \boldsymbol{\tau}_{C,part} \tag{5-7}$$

which result in the following control diagram:

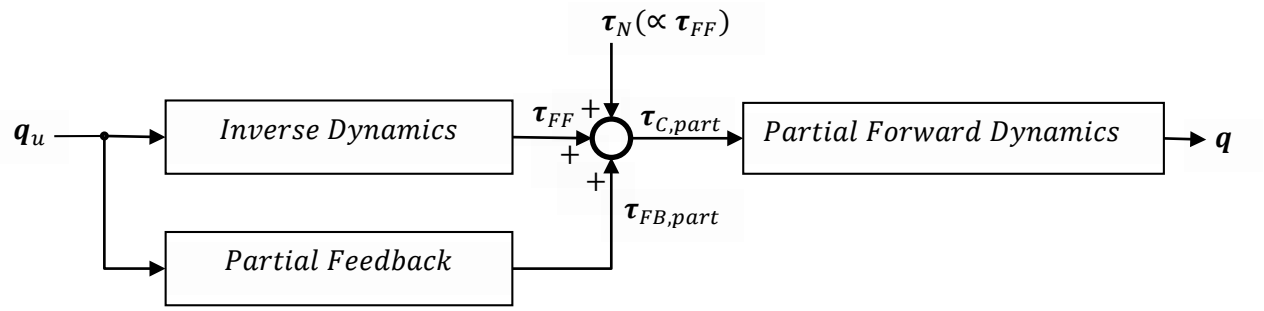


**Figure 5-3: Matlab Version of Control Diagram - Equivalent model of Figure 5-2 for use in Matlab to work with ode45 solver. Modified diagram courtesy of Dr. Charles.**

In the new Matlab diagram, inverse dynamics are the same, wrist and reaching partial feedback torque is $D_a\dot{\boldsymbol{q}}_u + K_a\boldsymbol{q}_u = \boldsymbol{\tau}_{FB,part}$, wrist partial forward dynamics is $I\ddot{\boldsymbol{q}} + \left(D_p + D_a\right)\dot{\boldsymbol{q}} + \left(K_p + K_a\right)\boldsymbol{q} = \boldsymbol{\tau}_{C,part}$ and reaching partial forward dynamics is $H\ddot{\boldsymbol{q}} + C\dot{\boldsymbol{q}} + D_a\dot{\boldsymbol{q}} + K_a\boldsymbol{q} = \boldsymbol{\tau}_{C,part}$.

For the wrist, parameters for mass, inertia, lengths, and "passive" stiffness and damping were taken from Charles and Hogan (2012), and the "active" parameters for proportional and derivative feedback gains were derived by using Halaki et al. (2006) values for FE, and scaling the other matrix values proportionally by the matrix of values in Charles and Hogan (2012). For the arm, all parameters were taken from Tee et al. (2004) and solved for using the methods described in Tee et al. (2004). Coefficients of variation for both wrist and reaching to simulate muscular noise were taken from de C. Hamilton et al. (2004). However, arm mechanical properties were extensively reviewed in literature, as found in Appendix E: Literature Review on Reaching Parameters Chart.

To get more consistent data, the sampling frequency was 1000Hz. 0.2 seconds of nonmoving data were added to the beginning and end of the data set in order to avoid introducing artifact to the signal due to filtering. The simulated data were filtered backward and

forward (using Matlab's filtfilt function) after each numerical differentiation after the forward dynamics with a 6th order Butterworth filter with 15Hz cut-off frequency. Noise was added as a normally distributed random signal amplified by the coefficient of variation, and was proportional to the feed-forward torque. The noise was scaled so that the ratio of the noise in the noisy $\boldsymbol{\tau}_{FF}$ signal to the mean of the noisy $\boldsymbol{\tau}_{FF}$ signal was equal to the coefficient of variation. I repeated the process on 5 movements to each target and direction (80 total trajectories) to reduce the standard deviation of the measures. The time step (1/sampling frequency), nonmoving pre- and post-data, and filtering were decided on by systematically reducing the numerical error of the process to be close as possible to a Jerk Ratio of 1 without noise (see Appendix F: Reduction of Numerical Error in Simulation).

### 5.2.2 Results of 1-2 Hypothesis

The simulation was verified by running inverse and forward dynamics without noise (which also included filtering and feedback), and the measures were accurate (NumMax was 1 and Jerk Ratio was between 1.03-1.10, which is just above 1 due to slight numerical error). For more explanation, see Appendix F: Reduction of Numerical Error in Simulation. The visual representation would look almost exactly like the equivalent minimum-jerk trajectory input (like Figure 5-4 and Figure 5-5 Min Jerk without noise) except for a filtered transition between the sharp jerk start and stop.

The result of the added noise from muscular variation only added a very small amount of noise to the trajectory (See Figure 5-4 and Figure 5-5). The measures from the minimum jerk trajectories with added noise were about 1/10th of the measures found in real data. Also, the speed profiles still closely resembled a minimum jerk trajectory with subtle waviness, where the real data resulted in large and distinct peaks which were not always symmetrical. Even from the

largest relative amounts of noise that result from movements requiring higher torque, this noise was too low to change the overall shape of the data.

The values for the mean and standard deviation of 5 iterations of all targets and directions (80 total trajectories) of the smoothness measures are listed in the table below (See Table 5-2).

**Table 5-2: Hypothesis 1-2 Smoothness Measures – Model of inverse and forward dynamics, with filtering, feedback torque, and muscular noise.**

| | | Jerk Ratio | | NumMax | |
|---|---|---|---|---|---|
| Duration | Joint | Mean | SD | Mean | SD |
| [illegible] | [illegible] | [illegible] | [illegible] | [illegible] | [illegible] |
| [illegible] | [illegible] | [illegible] | [illegible] | [illegible] | [illegible] |
| [illegible] | [illegible] | [illegible] | [illegible] | [illegible] | [illegible] |
| [illegible] | [illegible] | [illegible] | [illegible] | [illegible] | [illegible] |
| [illegible] | [illegible] | [illegible] | [illegible] | [illegible] | [illegible] |
| [illegible] | [illegible] | [illegible] | [illegible] | [illegible] | [illegible] |

I successfully modified the theoretical intended movement to include the noise. Adding the noise did not make theoretical movements comparable to the results of the actual data, so the hypothesis is false.

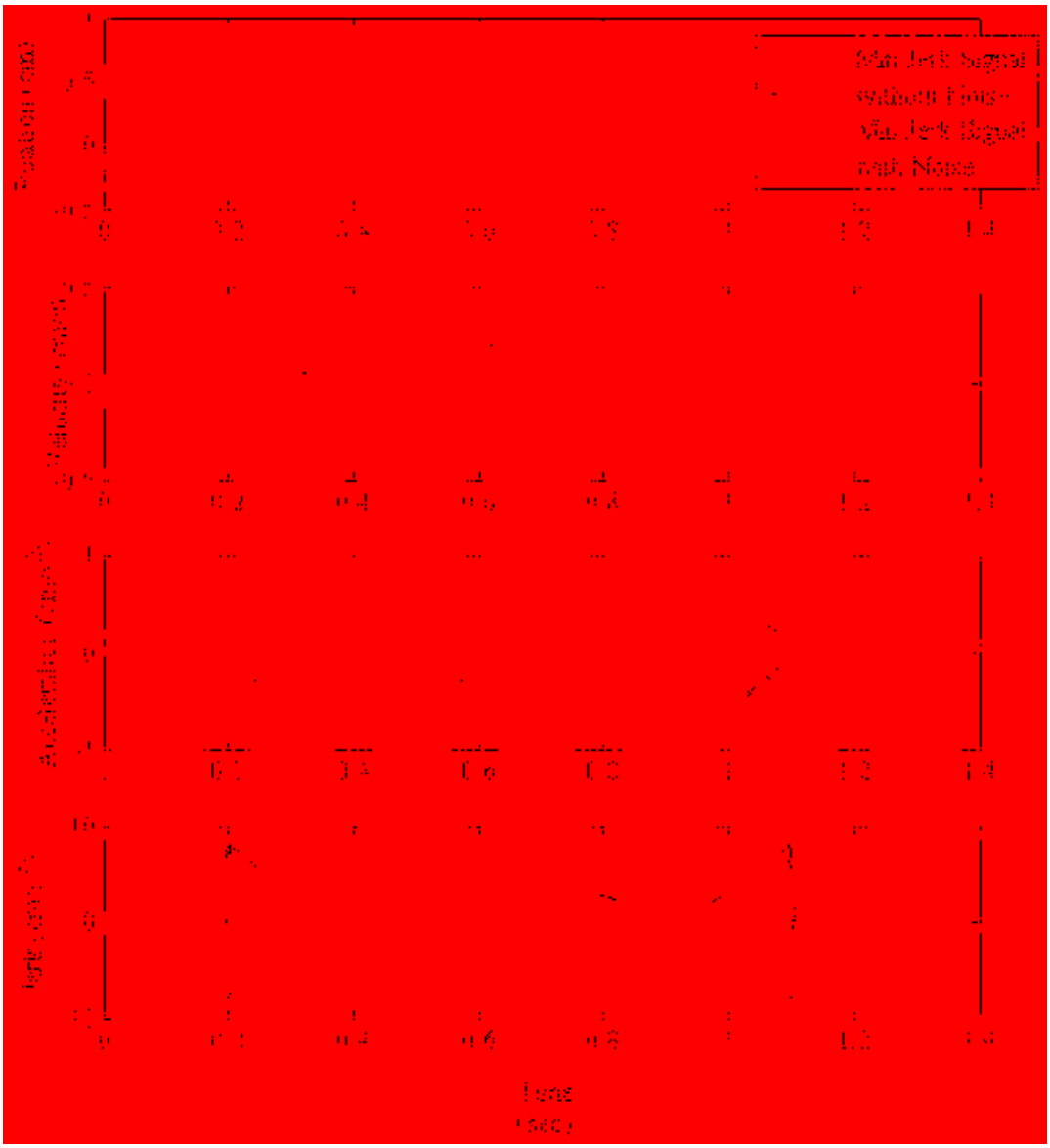

**Figure 5-4: Ideal Reach with Coefficient of Variation Noise - Sample 900ms reaching movement inbound from Target 8 with noise, feedback, and filtering when differentiated (15Hz cut-off frequency, 6$^{th}$ order).**

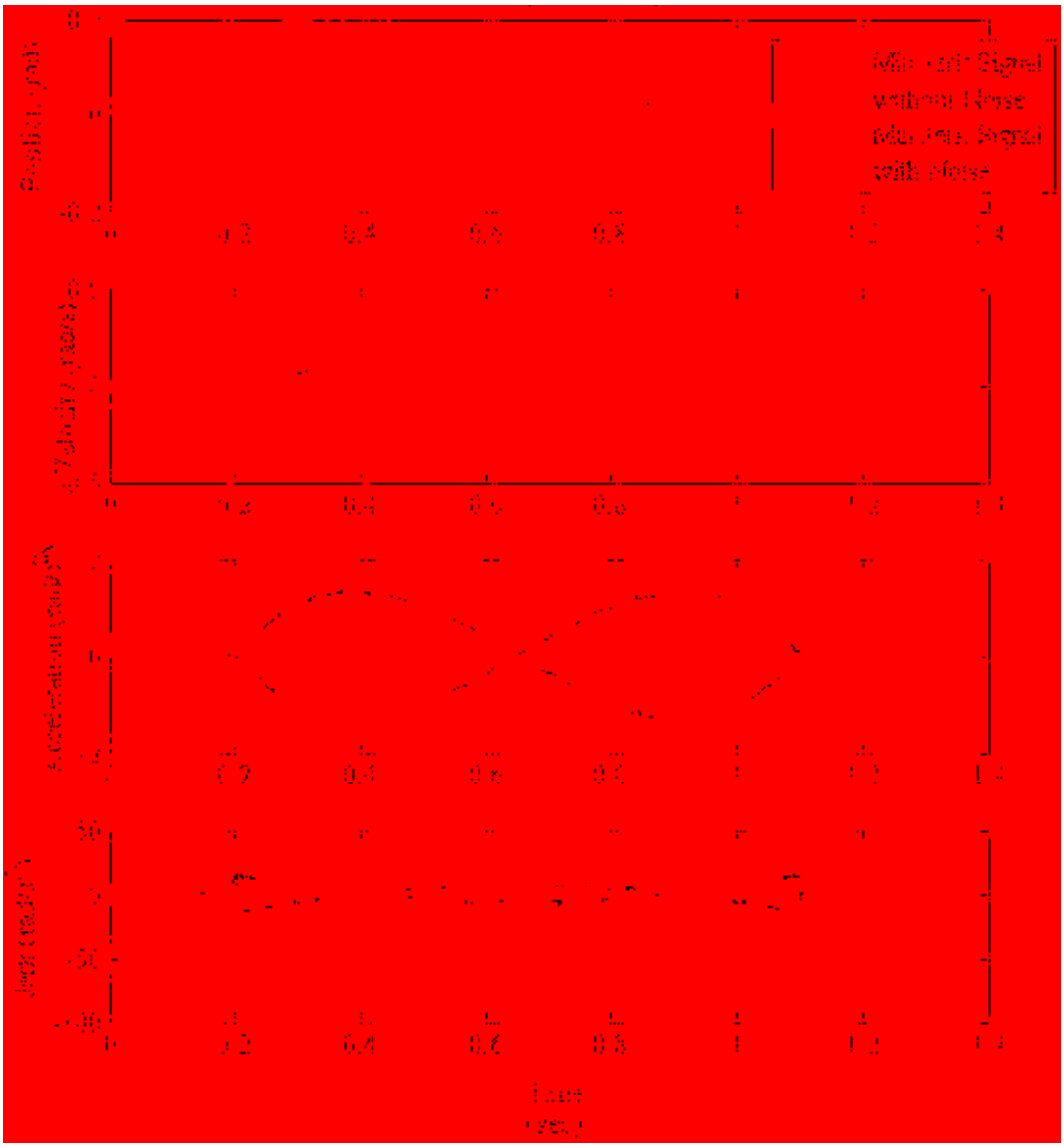

**Figure 5-5: Ideal Wrist with Coefficient of Variation Noise - Sample 900ms wrist movement inbound from Target 8 with noise, feedback, and filtering when differentiated (15Hz cut-off frequency, 6th order).**

## 5.3 Hypothesis 1-3: Neural Cause

Distal joints have less sensitive proprioception than proximal joints, which may be directly proportional to the smoothness of a movement. A distal joint (such as the wrist) would not sense its location accurately and would have more jerkiness when accounting for larger deviations than a more proximal joint.

To observe if this was the cause, I needed to find past research that shows what differences in proprioception exist between the wrist and the arm. If there were significant differences between the joints and it could explain why smoothness is different, then this hypothesis is true.

### 5.3.1 Test for 1-3 Hypothesis

I did a literature review of quantified proprioception at the joints and the implications of differing proprioception on smoothness.

### 5.3.2 Results of 1-3 Hypothesis

The literature review of this topic was difficult to find quantitative amounts of proprioception at certain joints. Jones and Lederman (2006) give a summary of proprioceptive properties from distal to proximal. To summarize, higher muscle spindle density (which assist with measuring proprioception) is found in muscles that are involved in fine movements (such as fingers), but this is not associated with better sensory acuity. There is no evidence indicating a superior acuity for detecting movements and changes in limb position as one goes from proximal to distal joints. However, proprioception may perform better in proximal joints than distal joints simply because the distal joints undergo greater displacement at the same angular rotation (Jones and Lederman, 2006).

Basically, literature review shows that proprioception is comparable at each joint of the arm, but (depending on your criteria) proprioceptive performance could show up as better at the shoulder/elbow joints or better at the hand/fingers joints (Hall and McCloskey, 1983). Because proprioception is not definitively better in one joint than the other, it is safe to say that the significant difference in smoothness would not be caused by this.

I found sufficient past research that shows differences in proprioception do not exist or are minimal at best between the wrist and the arm. There were no significant differences between the joints and it didn't explain why smoothness is different, so this hypothesis was false.

## 5.4 Hypothesis 1-4: Protocol Cause

Since I compared movements of like durations, the actual speed of each movement may actually not be equivalent. While the durations are the same, the movement amplitudes are not directly comparable since one is rotational and the other is linear, so the angular speed requirements may be different. Since smoothness is a function of speed, the apparent difference in smoothness could simply be a difference in speeds.

To observe if this was the cause, I needed to find the average angular speed of each task and target, and compare the speeds to the observed measures of smoothness. If the difference in angular speed causes the wrist movement smoothness measures converge with the reaching movement smoothness so the effect of angular speed on smoothness is shown to be independent of the joint, then this hypothesis is true.

### 5.4.1 Test for 1-4 Hypothesis

I compared wrist and reaching movements that have similar angular velocities (instead of duration) and tested whether the differences in smoothness remain. This analysis was performed on minimum-jerk data because the mean speed between two points with certain duration is the same whether the movement was smooth or not.

The analysis compares the two joints Jerk Ratio at each of the 8 targets at their respective angular speed. I also compared differences between the durations for reaching and wrist.

### 5.4.2 Results of 1-4 Hypothesis

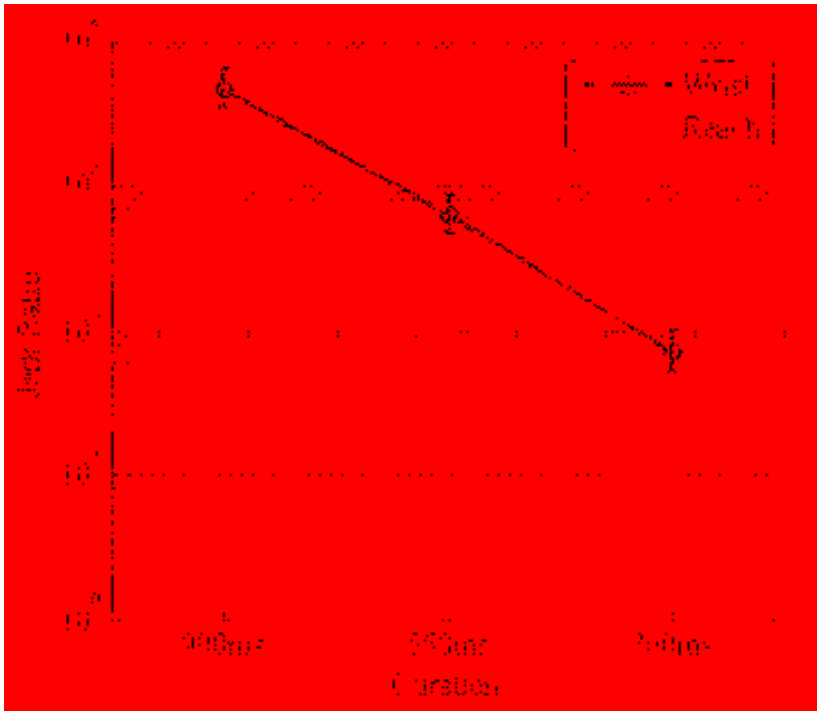

**Figure 5-6: Duration vs. Jerk Ratio - Plot of movement duration and Jerk Ratio (top left plot of Figure 4-4).**

Charles and Hogan (2010) argued that the similarities between the tasks makes reaching and wrist rotations comparable. While they are separate joints, there are both 2 degrees of freedom. Wrist rotation motion is essentially planar. In addition, the compared displacements of 14cm and 15° are justified by the same general of range of motion.

Based on Charles and Hogan (2010), the 300ms duration was chosen to be in the range of "as fast as possible", and the 550ms and 900ms were chosen to cover both ends of the large variation of movements "at a comfortable speed". However, the durations chosen needed justification from this test to find if the durations chosen elicited varying speeds that would affect smoothness.

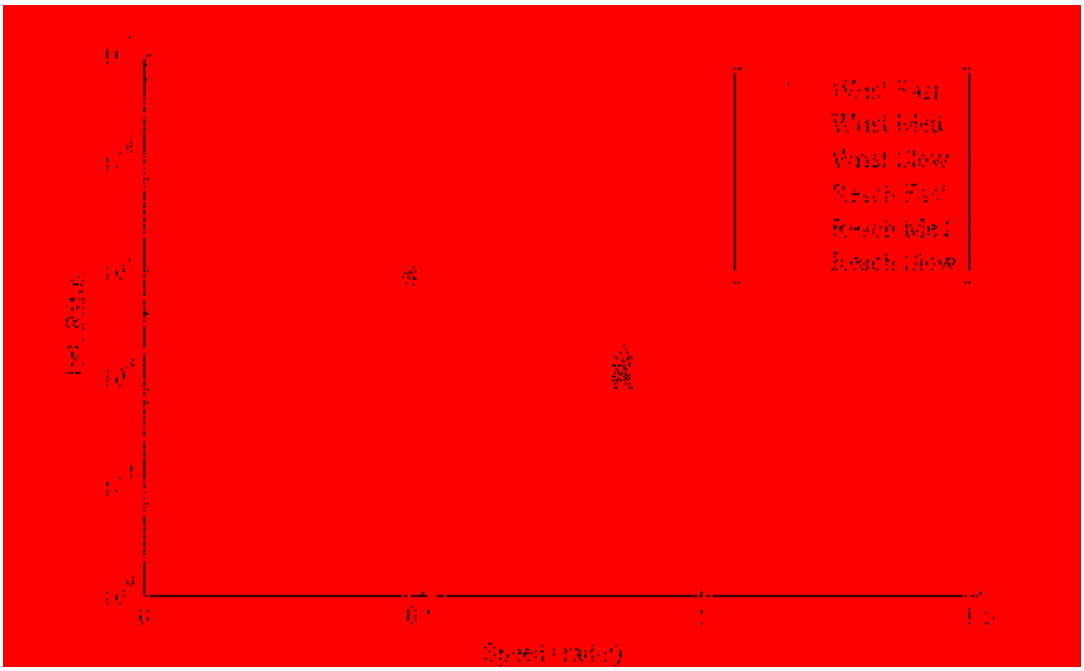

**Figure 5-7: Angular Speed vs. Jerk Ratio - Angular speed of wrist and reaching, and Jerk Ratio measure.**

Figure 5-7 is the angular speeds mixed with the reaching data per target. This is correlated to Figure 5-6. The method to find the reaching speed is $\frac{|q_1+q_2|+|q_1|}{2}$. The method to find wrist speed is $\sqrt{{q_1}^2+{q_2}^2}$.While the Jerk Ratio measure does vary at the duration for the wrist, the speed of the wrist rotations are constant. The Jerk Ratio measure for reaching movements does increase at the slower speeds, but the correlation is not consistent within the reaching targets. Some targets that require faster speeds are still on the same general horizontal trend line as the targets that require slower speeds.

I found the average angular speed of each task and target, and compared the speeds to the observed measures of smoothness. The difference in angular speed did not cause the wrist movement smoothness measures converge with the reaching movement smoothness, and the effect of angular speed on smoothness depended on the joint, so this hypothesis was false.

## 5.5 Hypothesis 3-1A: Neuromuscular System Anisotropy Cause

The fundamental assumption for the hypotheses listed under 3-1 is that an anisotropy in smoothness must be caused by an anisotropy in the neuromuscular system or in the execution of movements. The following hypotheses are based on this assumption and explore various anisotropies.

Specifically for Hypothesis 3-1A, there is anisotropy in the musculoskeletal dynamics of the wrist, which creates anisotropy in torque and secondarily anisotropy in signal-dependent noise. Since these properties change based on direction (Charles and Hogan, 2011, 2012), this may affect the signal-dependent noise and smoothness of the movement.

To observe if this was the cause, I needed to observe how the modeled wrist movement with noise affected direction. If the smoothness trends of the simulation correlated with those of the actual data, then this hypothesis is true.

### 5.5.1 Test for 3-1A Hypothesis

Compare variation in wrist musculoskeletal dynamics by modeling each direction's smoothness. We used the model created for hypothesis 1-2, and ran the model 100 times for each target and direction.

### 5.5.2 Results of 3-1A Hypothesis

To understand the effect of musculoskeletal dynamics vs. gravity, the effects of anisotropy in musculoskeletal dynamics without gravity and with gravity are explored separately. With noise but without gravity, the roughest simulated movements are to and from targets 4 and 8, which is close to the direction of greatest stiffness (which is 19° counterclockwise from the radial-ulnar deviation axis). However, if stiffness is the sole reason for this anisotropy in

smoothness, movements to and from targets 1 and 5 should be even a little noisier since they are even closer to the direction of greatest stiffness (see left subplot in Figure 5-8).

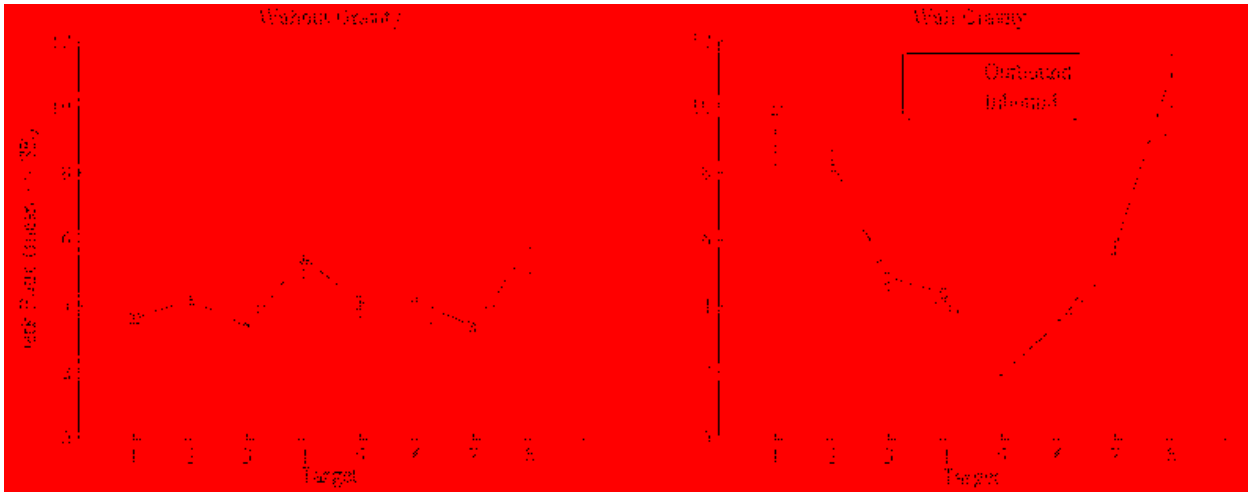

**Figure 5-8: Modeled Wrist Rotations, 3-1A – Jerk Ratio for the mean of 100 wrist movements with noise. Left subplot is without gravity, right subplot is with gravity.**

Although the gravity term is constant ($mgr$) and was thought to have a similar effect on all targets (at least pseudostatically), the simulations show that the presence of gravity creates considerable differences in smoothness between targets. This effect is likely due to whether gravity assists in accelerating or decelerating the movement, and hence whether most of the signal-dependent noise is added early or late in the movement. With noise and gravity, simulated movements to and from targets 1 and 8 are the noisiest, presumably because the torque in those directions is the largest because it has to overcome gravity and stiffness (see right subplot in Figure 5-8). In harmony with this speculation, movements to and from target 5 are the smoothest, presumably because stiffness partially compensates for gravity. Comparing the jerk ratio of movements with and without gravity, it is apparent that the effect of anisotropy in gravity dominates over the effect of anisotropy in stiffness.

The arguments in favor of this hypothesis (that differences in smoothness between targets are caused by differences in dynamics) are that 1) the pattern is roughly sinusoidal and 2)

roughly correct for inbound movements. However, the simulated movements show no separation between outbound and inbound movements, the pattern is completely incorrect for outbound movements, and the magnitude of the simulated jerk ratio is too low by two orders of magnitude.

I observed how the modeled wrist movement with noise affected direction. The smoothness trends of the simulation of inbound movements did correlate with those of the actual data, but the outbound did not correlate, so this hypothesis was false.

## 5.6 Hypothesis 3-1B: System Anisotropy with Step Input Cause

This variation on hypothesis 3-1A is similar, but it assumes a step input in torque instead of minimum-jerk desired trajectory. For an underdamped system, a step input in torque will create overshoot and oscillations, which may be the submovements observed in the speed profiles. A step input in torque has been used successfully to model wrist movements in the past, like as in Charles and Hogan (2012).

To observe if this was the cause, I needed to modify the 3-1A model to include a step input. If the smoothness trends of the simulation correlated with those of the actual data, then this hypothesis is true.

### 5.6.1 Test for 3-1B Hypothesis

Perform the same test as done in hypothesis 3-1A, except change the minimum-jerk desired trajectory into a step input.

### 5.6.2 Results of 3-1B Hypothesis

The results of this test did produce a pattern that is roughly sinusoidal (See Figure 5-9). However, there are many arguments against this hypothesis. The resulting trajectory does not

look like the observed trajectory, especially in acceleration and jerk (See Figure 5-10). Also, the roughly sinusoidal pattern has twice the frequency of the observed frequency. There is slight separation between outbound and inbound movements, but the roughly sinusoidal patterns are in phase. Assuming a step input completely constrains the movement duration to a single value for each target (so the resulting patterns for fast, medium, and slow movements are identical except for noise). Finally, the magnitude of the simulated jerk ratio is too low by two orders of magnitude. This hypothesis, therefore, is not a viable explanation for the observed difference in smoothness between targets.

I successfully modified the 3-1A model to include a step input. The smoothness trends of the simulation did not correlate with those of the actual data, so this hypothesis is false.

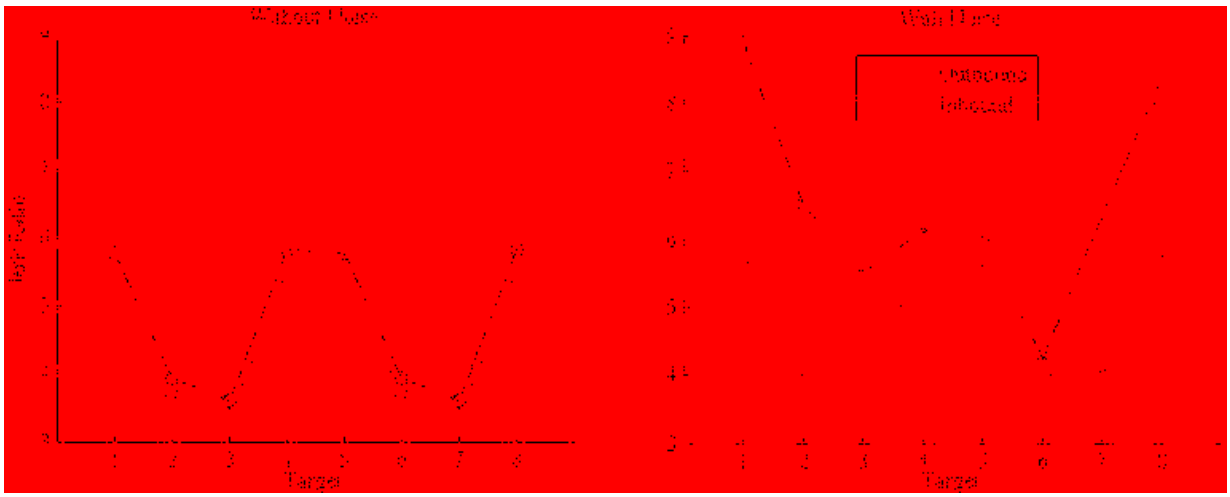

**Figure 5-9: Modeled Wrist Rotations, 3-1B – Jerk Ratio for step input wrist movements with gravity. Left subplot is without noise, right subplot is of the mean ± SE of 100 movements with noise.**

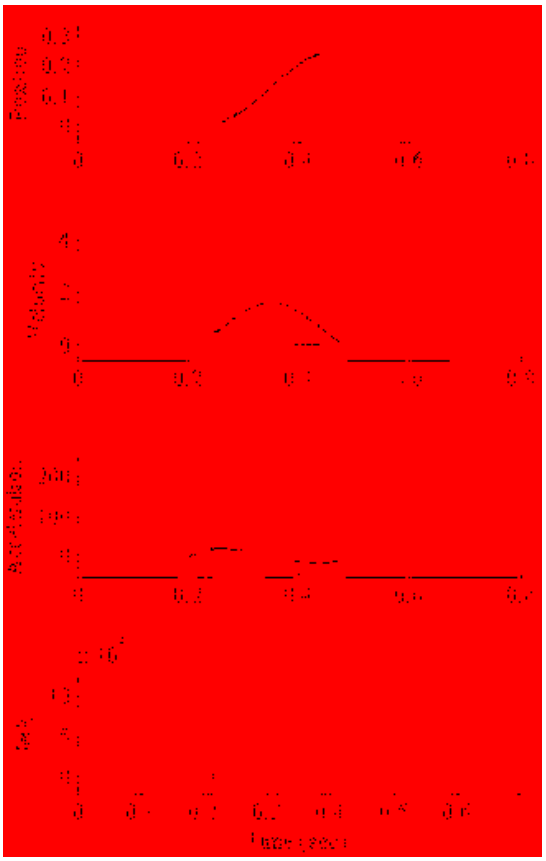

**Figure 5-10: Trajectory for Step Input Torque – Trajectory in task space to Target 1 for 300ms wrist movement. Blue is minimum jerk trajectory, red is step input trajectory**

## 5.7 Hypothesis 3-1C: System Anisotropy with Low Damping Cause and Test

This variation on hypothesis 3-1B is similar, but it assumes a lower damping ratio. The damping ratio resulting from the passive impedance parameters used in our simulation is 0.63 (FE) and 0.74 (RUD). Investigations of human movement have often found lower damping ratios. For example, Halaki et al. (2006) found 6° wrist movements in FE to have a damping ratio of 0.14.

To observe if this was the cause, I needed to modify the 3-1B model to include a lower damping ratio. If the smoothness trends of the simulation correlated with those of the actual data, then this hypothesis is true.

### 5.7.1 Test for 3-1C Hypothesis

We repeated the simulation from hypothesis 3-1B, but with the damping and stiffness matrices from Halaki et al. (2006) (i.e. we assigned $D_p$ and $K_p$ to be the same as $D_a$ and $K_a$), resulting in a damping ratio of 0.14.

### 5.7.2 Results of 3-1C Hypothesis

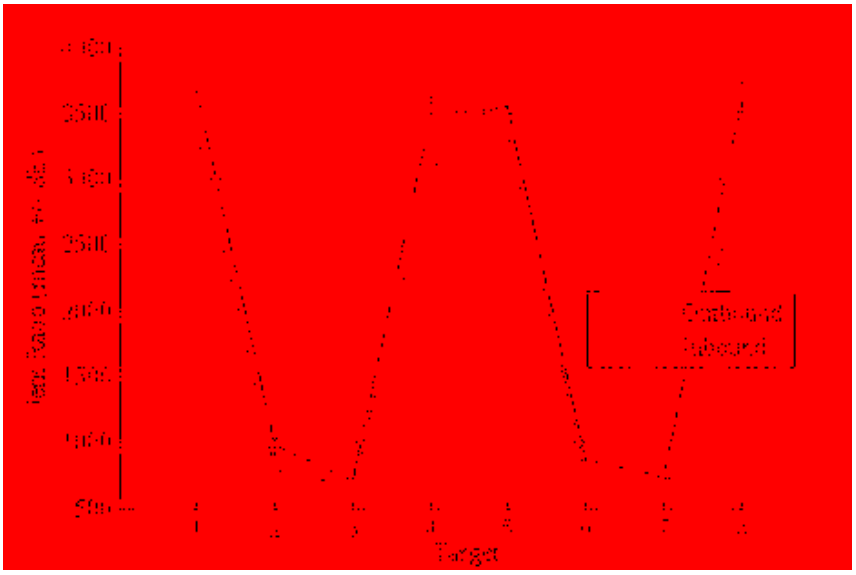

**Figure 5-11: Modeled Wrist Rotations, 3-1C – Jerk Ratio for the mean of 100 step torque input wrist movements with noise, gravity, and low damping ratio (0.14).**

The arguments for this hypothesis is that the pattern is sinusoidal (See Figure 5-11), and the jerk ratio has the right order of magnitude. However, the arguments against this hypothesis are the same as for hypothesis 3-B (except magnitude of jerk ratio). Therefore, this hypothesis also fails to be a viable explanation for the observed difference in smoothness between targets.

I modified the 3-1B model to include a lower damping ratio. The smoothness trends of the simulation did not correlate with those of the actual data, so this hypothesis is false.

## 5.8 Hypothesis 3-2: Anisotropy in Movement Duration Cause and Test

Anisotropy of smoothness measures is due to varying movement duration between targets. Longer durations are associated with greater jerk ratio, so if there is variation in duration, then this may account for varying smoothness.

To observe if this was the cause, I needed to find the average duration of each direction of movement. If the longer duration movements correlated with higher jerkiness and vice versa, then this hypothesis is true.

### 5.8.1 Test for Hypothesis 3-2

We separated the target and directions by the duration of each movement and visually compared the durations with the smoothness. We explored if there is a correlation between smaller durations and better smoothness measures.

### 5.8.2 Results of 3-2 Hypothesis

This hypothesis fit the actual data fairly well (See Figure 5-12). The main argument in favor of this hypothesis is that the pattern of duration is roughly the same as the pattern in the jerk ratio. More specifically, the pattern in duration is roughly sinusoidal, with the correct frequency, the outbound and inbound patterns are roughly 180° out-of-phase, and the outbound and inbound patterns of duration are roughly in-phase with the outbound and inbound patterns of jerk ratio, so movements with greater duration have greater jerk ratio. Also, the jerk ratio is known to be highly sensitive to movement duration, so this hypothesis makes logical sense.

The only argument against this hypothesis is that the duration of outbound movements to targets 1 and 2 is relatively long compared to their low jerk ratio values.

I found the average duration of each direction of movement. The longer duration movements usually did correlate with higher jerkiness and vice versa, so this hypothesis is true.

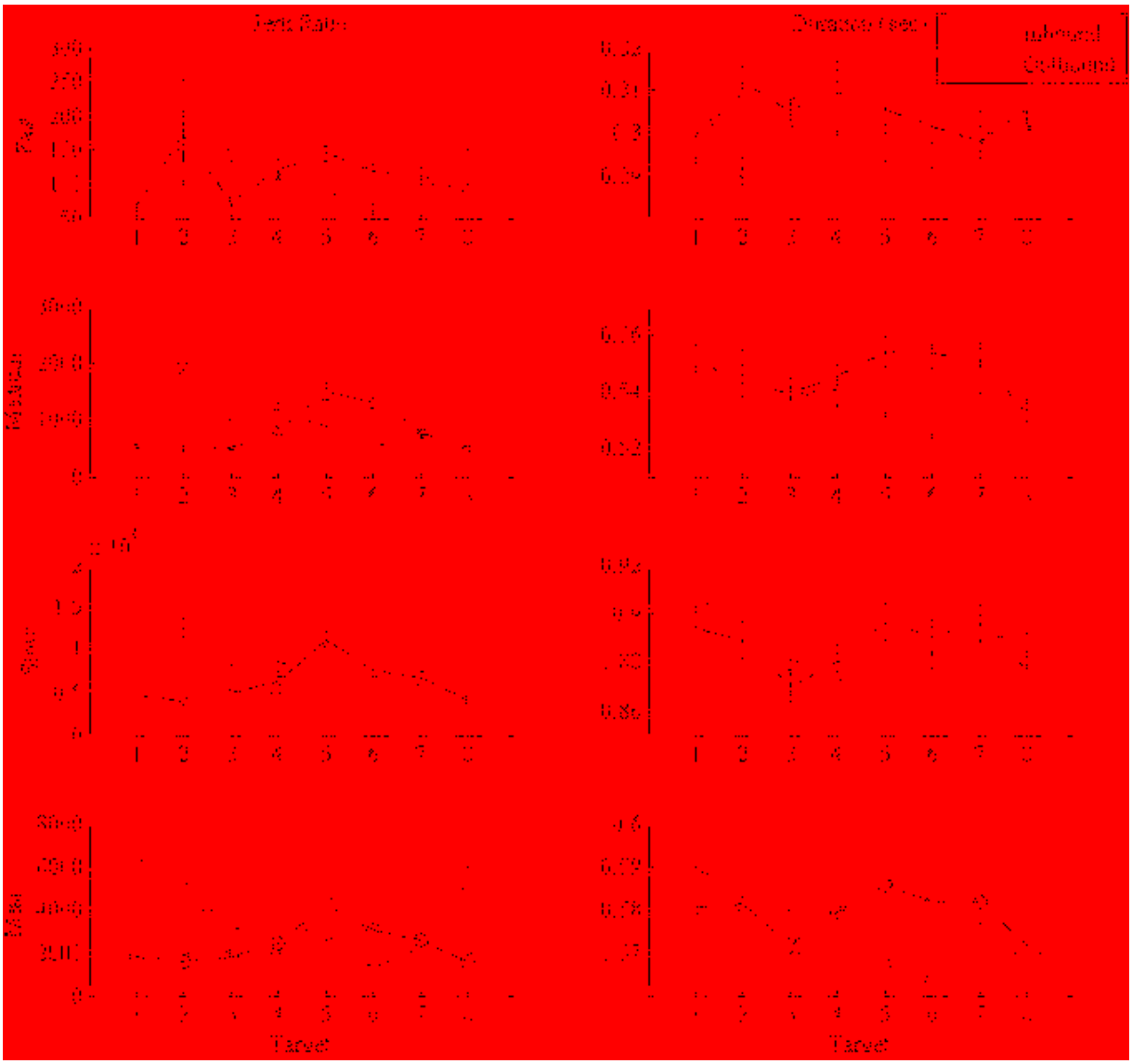

**Figure 5-12: Actual Wrist Smoothness and Durations – Left subplot is Jerk Ratio, right subplot is Duration.**

# 6 DISCUSSION

The purpose of this research was to characterize the smoothness of healthy wrist rotations and compare them to the baseline of healthy reaching movements, quantify smoothness of the data, and explore underlying differences in smoothness. The study explored how smoothness differs between joints, speeds of wrist rotation, and movement direction. To quantify smoothness, this study used an established method (quantifying the number of maxima, or NumMax) and uncovered a novel method (creating a comparison of the movement's jerk to its equivalent minimum-jerk trajectory, or Jerk Ratio). The results of this study found that wrist rotations are significantly less smooth than reaching movements ($p \leq 0.0016$), faster wrist rotations are significantly smoother than slower wrist rotations ($p < 0.0001$), and smoothness varies with movement direction in a predictable pattern.

## 6.1 Causes Underlying the Major Findings

To test possible reasons behind the major findings, simulations and tests were performed to try possible reasons for each major finding. For a review of the hypotheses and their respective tests, please review Chapter 5.

### 6.1.1 Discussion of Finding 1

This study is the first report of a difference in smoothness between wrist and reaching movements.

Concerning the hypotheses that were tested in this study, the most promising explanation for why wrist rotations are jerkier than reaching movements is due to the mechanical properties of the joints. The impedance properties (inertia, damping, and stiffness) of the shoulder and elbow give the arm a smaller bandwidth than the wrist. This additional noise may be important to understand for the smoothness measure to be applied to practical settings.

The study did rule out some possible explanations. The signal-dependent noise that is part of muscle force may be a contributor to the overall jerky signal of a movement, but is too small to be the sole cause. This noise for the wrist would need to be amplified by an order of magnitude before it would begin to resemble the actual observed trajectories, but it would still not cause the variation of not blended peaks that is predominantly found in wrist rotations. The noise for reaching movements would need to be amplified by two orders of magnitude to begin to resemble the actual observed trajectories.

The confirmation that the joint speeds were fairly similar between the wrist and reaching movements helped verify that the comparison between reaching and wrist movement by certain durations was appropriate. This also shows that while speed does play a role in smoothness, certain speeds that varied by target did not correlate with the varying smoothness as much as the relative speed to the subject's level of comfort with the movement.

Proprioception of the limb is not the source of jerkiness because there is no correlation between them. Literature reveals that proprioception is not very quantifiable, nor is it as simple as saying one joint is better than another. The differences in smoothness that we see in the results

don’t seem related to one’s proprioception performance since there doesn’t seem to be a difference.

### 6.1.2 Discussion of Finding 3

The differences in smoothness of wrist rotations between movement directions can be fairly well simulated by observing the differences between movement duration between directions. However, this does leave some other questions to look into that would be future work. Before ensuring this is the underlying cause, one would need to determine if the differences in duration between directions is statistically significant, and determine why there is a difference in movement duration. Also, according to the observed pattern, outbound movements to targets 1 and 2 take longer than they should, so the reasoning should be explored.

While we know from hypothesis 1-4 that the difference between wrist and reaching durations are very small, we may want to check if this explains the difference between them. Also, it may be helpful to test to see if there is a correlation between duration and jerk ratio within a target and duration category. Finally, it would be important to explore if the change in jerk ratio with movement duration (i.e. the sensitivity, or slope) seen within a duration category is similar to that seen between duration categories.

## 6.2 Limitations of Findings

When calculating the reaching angular speed for hypothesis 1-4, the method for combining the shoulder and elbow speeds were an approximation. A few other methods were considered for calculating reaching angular speed, as well as averages of multiple methods. However, this method made the most sense intuitively and made a decent approximation for our purposes.

While durations were kept constant and mean speeds were similar, the instructions for the subject to make movements "straight and continuous" were not enforced by the protocol. From my observations, subjects tried to have straight and continuous movements, but any movements that may have been stop-and-go still could be used in the data if it was within the right duration.

For this study, I only looked at two measures of smoothness. There are many other measures of smoothness that may be more robust or provide additional insight. For example, Balasubramanian et al. (2012) analyzes about 8 metrics used for quantifying smoothness, including peaks and dimensionless jerk, and argues that there are more robust ways to measure smoothness. Also, Rohrer et al. (2002) evaluates the accuracy of smoothness measures according to the blending of submovements. However, for the purposes of this study, I chose measures that were more intuitive in meaning, and I altered the dimensionless jerk measure to be more intuitive.

While I did try to reduce artifact of the filter on the data, the choice of filter left important characteristics of the movements alone while avoiding unnecessary noise. Filtering was necessary to obtain the Jerk Ratio measure. The filtering did affect the measures, but did not change the overall findings. However, this noise that I neglected may have additional implications for these movements.

To more conclusively test our hypothesis, there are other possible tests that could be explored. For example, adding mass to wrist to see if movement is smoother from higher inertia (Krylow and Rymer, 1997) would further confirm Hypothesis 1-1.

## 6.3 Conclusion

These findings are very robust (extremely low p-values—see Table 4-1) and confirm my hypothesis: Wrist movements are much less smooth than reaching movements. These findings

help us better understand the smoothness of wrist movements, and help better understand important characteristics of movements in health and disease. This understanding deepens our fundamental understanding of motor neuroscience and will allow us to improve the diagnosis and rehabilitation of neurological disorders.

To test the effectiveness of the measures, one could apply the measures of smoothness to monitoring devices and using these monitors to improve physical therapy practices on patients with movement disorders, such as stroke. By programming a rehabilitation robot to track these measures, games could be designed specifically to improve those measures. Also, attempting to use these measures on mobile monitoring devices may help clinicians understand the effect of therapy on the patient's Activities of Daily Living at home. This feedback could also be used in applications such as improving handling skills and preventing work injuries or repetitive strain injuries.

Future work to expand on the hypotheses would also be beneficial for improving the underlying causes of the findings. For hypothesis 1-1, the power found in the wrist movement power spectrum can be further explored to identify if the difference band is substantial enough to cause the findings, and whether the reaching movements have that noise (filtered out) or not. For hypothesis 1-2, the model could be improved to also include feedback delay and submovements. For hypothesis 1-3, other neurological differences between each joint could be explored and tested. For hypothesis 1-4, other aspects of the protocol could be explored for reasons of jerkiness, such as letting the subject move at their own comfortable speeds. For hypothesis 3-1, the correlation of the model with gravity could be further explored since it made a model's inbound trend accurate, but not the outbound. For hypothesis 3-2, whether the difference in

duration is significant should be explored, and the reasons for the differences would be important.

As stated previously, the purpose of this study was to characterize the smoothness of wrist rotations so smoothness could be used as a marker for diagnosis and evaluation, similarly to the characterization that exists for reaching movements. This study established methodology, appropriate filtering properties, measures of smoothness, statistically significant differences between factors, and explored the explanation of these differences. The information provided here is new information for wrist research, and can be used to evaluate the behavior of the wrist and diagnose unhealthy and abnormal wrist rotation, and improved our current understanding of the wrist and its many mysteries.

## REFERENCES


**Atkeson CG, Hollerbach JM**. Kinematic features of unrestrained vertical arm movements. *The Journal of Neuroscience* 5: 2318, 1985.

**Balasubramanian S, Melendez-Calderon A, Burdet E**. A robust and sensitive metric for quantifying movement smoothness. *Biomedical Engineering, IEEE Transactions on* 59: 2126–2136, 2012.

**Bennett D, Hollerbach J, Xu Y, Hunter I**. Time-varying stiffness of human elbow joint during cyclic voluntary movement. *Experimental Brain Research* 88: 433–442, 1992.

**Bennett DJ**. Torques generated at the human elbow joint in response to constant position errors imposed during voluntary movements. *Experimental Brain Research* 95: 488–498, 1993.

**Brooks V, Cooke J, Thomas J**. The continuity of movements. In: *Control of posture and locomotion*. Springer, 1973, p. 257–272.

**Burdet E, Franklin DW, Milner TE**. *Human Robotics: Neuromechanics and Motor Control*. MIT Press, 2013.

**Burdet E, Osu R, Franklin D, Yoshioka T, Milner T, Kawato M**. A method for measuring endpoint stiffness during multi-joint arm movements. *Journal of Biomechanics* 33: 1705–1709, 2000.

**De C. Hamilton AF, Jones KE, Wolpert DM**. The scaling of motor noise with muscle strength and motor unit number in humans. *Experimental Brain Research* 157: 417–430, 2004.

**Charles SK, Hogan N**. The curvature and variability of wrist and arm movements. *Experimental Brain Research* 203: 63–73, 2010.

**Charles SK, Hogan N**. Dynamics of wrist rotations. *Journal of Biomechanics* 44: 614–621, 2011.

**Charles SK, Hogan N**. Stiffness, not inertial coupling, determines path curvature of wrist motions. *Journal of Neurophysiology* 107: 1230–1240, 2012.

**Charles SK**. It's all in the wrist: a quantitative characterization of human wrist control. *Massachusetts Institute of Technology, PhD Thesis* 2008.

**Dipietro L, Krebs HI, Fasoli SE, Volpe BT, Hogan N**. Submovement changes characterize generalization of motor recovery after stroke. *Cortex* 45: 318–324, 2009.

**Doeringer JA, Hogan N**. Intermittency in preplanned elbow movements persists in the absence of visual feedback. *Journal of Neurophysiology* 80: 1787–1799, 1998.

**Fetters L, Todd J**. Quantitative assessment of infant reaching movements. *Journal of Motor Behavior* 19: 147–166, 1987.

**Flash T, Hogan N**. The coordination of arm movements: an experimentally confirmed mathematical model. *Journal of Neuroscience* 5: 1688–1703, 1985.

**Flash T, Mussa-Ivaldi F**. Human arm stiffness characteristics during the maintenance of posture. *Experimental Brain Research* 82: 315–326, 1990.

**Franklin DW, Liaw G, Milner TE, Osu R, Burdet E, Kawato M**. Endpoint stiffness of the arm is directionally tuned to instability in the environment. *Journal of Neuroscience* 27: 7705–7716, 2007.

**Franklin DW, So U, Kawato M, Milner TE**. Impedance control balances stability with metabolically costly muscle activation. *Journal of Neurophysiology* 92: 3097–3105, 2004.

**Gomi H, Kawato M**. Human arm stiffness and equilibrium-point trajectory during multi-joint movement. *Biological Cybernetics* 76: 163–171, 1997.

**Gomi H, Osu R**. Task-dependent viscoelasticity of human multijoint arm and its spatial characteristics for interaction with environments. *Journal of Neuroscience* 18: 8965–8978, 1998.

**Halaki M, O'Dwyer N, Cathers I**. Systematic nonlinear relations between displacement amplitude and joint mechanics at the human wrist. *Journal of Biomechanics* 39: 2171–2182, 2006.

**Hall LA, McCloskey D**. Detections of movements imposed on finger, elbow and shoulder joints. *Journal of Physiology* 335: 519–533, 1983.

**Harris CM, Wolpert DM**. Signal-dependent noise determines motor planning. *Nature* 394: 780–784, 1998.

**Hoffman DS, Strick PL**. Step-tracking movements of the wrist in humans. I. Kinematic analysis. *Journal of Neuroscience* 6: 3309, 1986.

**Hogan N, Krebs HI, Rohrer B, Palazzolo JJ, Dipietro L, Fasoli SE, Stein J, Hughes R, Frontera WR, Lynch D, others**. Motions or muscles? Some behavioral factors underlying robotic assistance of motor recovery. *Journal of Rehabilitation Research and Development* 43: 605, 2006.

**Hogan N, Sternad D**. Sensitivity of smoothness measures to movement duration, amplitude, and arrests. *Journal of Motor Behavior* 41: 529–534, 2009.

**Hogan N**. Adaptive control of mechanical impedance by coactivation of antagonist muscles. *Automatic Control, IEEE Transactions on* 29: 681–690, 1984.

**Jones LA, Lederman SJ**. *Human Hand Function*. Oxford University Press, 2006.

**Kahn L, Zygman M, Rymer W, Reinkensmeyer D**. Effect of robot-assisted and unassisted exercise on functional reaching in chronic hemiparesis. In: *Engineering in Medicine and Biology Society, 2001. Proceedings of the 23rd Annual International Conference of the IEEE*. 2001, p. 1344–1347.

**Krebs HI, Volpe BT, Williams D, Celestino J, Charles SK, Lynch D, Hogan N**. Robot-aided neurorehabilitation: a robot for wrist rehabilitation. *Neural Systems and Rehabilitation Engineering, IEEE Transactions on* 15: 327–335, 2007.

**Krylow AM, Rymer WZ**. Role of intrinsic muscle properties in producing smooth movements. *Biomedical Engineering, IEEE Transactions on* 44: 165–176, 1997.

**Kwakkel G, Kollen BJ, Krebs HI**. Effects of robot-assisted therapy on upper limb recovery after stroke: a systematic review. *Neurorehabilitation and Neural Repair* 22: 111–121, 2008.

**Lacquaniti F, Licata F, Soechting J**. The mechanical behavior of the human forearm in response to transient perturbations. *Biological Cybernetics* 44: 35–46, 1982.

**MacKay W, Crammond D, Kwan H, Murphy J**. Measurements of human forearm viscoelasticity. *Journal of Biomechanics* 19: 231–238, 1986.

**Mann KA, Wernere FW, Palmer AK**. Frequency spectrum analysis of wrist motion for activities of daily living. *Journal of Orthopaedic Research* 7: 304–306, 1989.

**Milner TE**. Dependence of elbow viscoelastic behavior on speed and loading in voluntary movements. *Experimental Brain Research* 93: 177–180, 1993.

**Morasso P**. Spatial control of arm movements. *Experimental Brain Research* 42: 223–227, 1981.

**Mussa-Ivaldi FA, Hogan N, Bizzi E**. Neural, mechanical, and geometric factors subserving arm posture in humans. *Journal of Neuroscience* 5: 2732–2743, 1985.

**Rohrer B, Fasoli S, Krebs HI, Hughes R, Volpe B, Frontera WR, Stein J, Hogan N**. Movement smoothness changes during stroke recovery. *Journal of Neuroscience* 22: 8297–8304, 2002.

**Rohrer B, Fasoli S, Krebs HI, Volpe B, Frontera WR, Stein J, Hogan N, others**. Submovements grow larger, fewer, and more blended during stroke recovery. *Motor Control* 8: 472–483, 2004.

**Selen LP, Franklin DW, Wolpert DM**. Impedance control reduces instability that arises from motor noise. *Journal of Neuroscience* 29: 12606–12616, 2009.

**Shadmehr R, Mussa-Ivaldi FA**. Adaptive representation of dynamics during learning of a motor task. *Journal of Neuroscience* 14: 3208–3224, 1994.

**Stroeve S**. Impedance characteristics of a neuromusculoskeletal model of the human arm I. Posture control. *Biological Cybernetics* 81: 475–494, 1999.

**Tee K, Burdet E, Chew C, Milner T**. A model of force and impedance in human arm movements. *Biological Cybernetics* 90: 368–375, 2004.

**Tee KP, Franklin DW, Kawato M, Milner TE, Burdet E**. Concurrent adaptation of force and impedance in the redundant muscle system. *Biological Cybernetics* 102: 31–44, 2010.

**Tsuji T, Goto K, Moritani M, Kaneko M, Morasso P**. Spatial characteristics of human hand impedance in multi-joint arm movements. In: *Intelligent Robots and Systems' 94.'Advanced Robotic Systems and the Real World', IROS'94. Proceedings of the IEEE/RSJ/GI International Conference on*. 1994, p. 423–430.

**Tsuji T, Morasso PG, Goto K, Ito K**. Human hand impedance characteristics during maintained posture. *Biological Cybernetics* 72: 475–485, 1995.

**Tsuji T, Takeda Y, Tanaka Y**. Analysis of mechanical impedance in human arm movements using a virtual tennis system. *Biological Cybernetics* 91: 295–305, 2004.

**Vallbo A, Wessberg J**. Organization of motor output in slow finger movements in man. *The Journal of Physiology* 469: 673–691, 1993.

**Wu G, Van der Helm FCT, Veeger H, Makhsous M, Van Roy P, Anglin C, Nagels J, Karduna AR, McQuade K**. ISB recommendation on definitions of joint coordinate systems of various joints for the reporting of human joint motion-Part II: shoulder, elbow, wrist and hand. *Journal of Biomechanics* 38: 981–992, 2005.

## APPENDIX A: PARTICIPANT DATA SHEET

CONFIDENTIAL

### BYU NML Participant Data Sheet

*Lab Use Only*

Experimenter(s): _____

Experiment Date/Time: _____/_____/_____ _____:_____am/pm -- _____:_____am/pm

Experiment Title: _____

File Code: _____

Name: _____

Sex: M F

Date of Birth (mm/dd/yyyy): _____/_____/_____

Race:

- ☐ White
- ☐ Black/African American
- ☐ Asian
- ☐ Hawaiian Native or Pacific Islander
- ☐ Native American or Alaska Native

Ethnicity:

- ☐ Hispanic or Latino
- ☐ NOT Hispanic or Latino

Weight: _____lbs

Height: _____ft _____in

Handedness: RH LH

Are you Color Blind? Y N

Do you have any pain in your upper limbs? Y N
If yes, describe:

Do you have any implanted devices? Y N
If yes, describe:

Do you have any medical conditions that affect motor-control/motion? Y N
If yes, describe:

Do you take any medications that affect motor-control/motion? Y N
If yes, describe:

## APPENDIX B: EXPERIMENT PROTOCOL



### SUBJECT INFORMATION

- ☐ File Code: _____
- ☐ Today's Date (mm/dd/yy): ____/____/____
- ☐ Subject is moderately well-rested? Yes No
- ☐ Subject wearing their glasses/contacts? Yes N/A
- ☐ Subject used restroom (if needed)? Yes N/A
- ☐ Pilot test? Yes No

### SET UP PRIOR TO SUBJECT ARRIVAL

**Environment**

- ☐ Room has been reserved
- ☐ Door is closed with Do Not Disturb sign on it
- ☐ Other noises in the room are minimized
- ☐ Curtains are closed
- ☐ Testing space is clear of clutter
- ☐ Metallic items are as far as possible
- ☐ Get out EDGE Magazines for break

**Settings**

- ☐ Computer and TrakSTAR are running with files easily accessible
- ☐ All other programs are closed
- ☐ Monitors are correctly placed and oriented
- ☐ Desktop background is a solid color

**Testing Setup**

- ☐ Place test materials in correct position
- ☐ Print Consent form, Subject Data Sheet & Contact Consent, and Protocol Checklist
- ☐ Randomized sequence written on protocol
- ☐ Open 1st correct random setting file
- ☐ Correct sensor is plugged in
- ☐ Layout black foam padding for the wrist apparatus

## WHEN SUBJECT ARRIVES

**Overview**

- ☐ Fill out Subject Information section
- ☐ Consent form
  - Explain and sign
  - Will make small dots with pen on subject's skin, unless prefer stickers
  - Would they like to keep a copy?
- ☐ Explain rules
  - You will move your wrist or arm over 160 times per test at three different speeds:
    - 300ms, which is fast speed; 75ms tolerance
    - 550ms, which is comfortable; 100ms tolerance
    - 900ms, which is slow; 150ms tolerance
  - Show Display Screen Tutorial PowerPoint Presentation
  - No talking during sessions (okay during breaks), tempo noises are okay
  - Questions about test purpose and hypothesis can be answered after completion
- ☐ Have subject remove metal from pockets and person
- ☐ Ask if there are any questions/comments: _____

**Wrist Positioning**

- ☐ Axes' points are located and marked
- ☐ Subject is sitting all the way back in the center of the chair and is facing forward
- ☐ Set up arm with approx. angles (0° abduction/45° arm radial/135° elbow flexion)
- ☐ Chair is at the right height and locked
- ☐ Chair is at the right position on the floor
- ☐ The wrist constraint apparatus is fastened moderately tight (subject tightens it himself/herself such that it is tight but does not affect wrist motion)
- ☐ Ask subject if he/she is comfortable
- ☐ Axes' points are lined up with laser level

**Arm Positioning**

- ☐ Subject is sitting all the way back in the center of the chair and is facing forward
- ☐ Set up arm with correct angles (90° abduction/45° arm radial/90° elbow flexion)
- ☐ Sling is at the right height
- ☐ Chair is at the right position on the floor
- ☐ Shoulder belts are fastened
- ☐ Measure around their wrist (Brace transition at 19cm) _____cm S/M L
- ☐ Correct size wrist brace is put on
- ☐ Make a loop with the cord around the forearm strap to give it some slack
- ☐ Ask subject if he/she is comfortable

## SUBJECT TESTING

**Before each test**

- ☐ Open correct random setting file
- ☐ Correct sensor is plugged in
- ☐ Data will be logged in file labeled (filecode)(w/r)(300/550/900).txt
- ☐ Wrist/Arm is in neutral position when position reading is zeroed
- ☐ Chair in correct position
- ☐ Place tape to mark location
- ☐ Make notes on this page for unique things that happened

**Record movements** (.075/.1/.15 sec tolerance)

- ☐ Start Time: _____
- ☐ Phase 1 300/550/900 Wrist/Reach
- ☐ 3 min Break and Set up for next test Approx. Moves: _____
- ☐ Phase 2 300/550/900 Wrist/Reach
- ☐ 3 min Break and Set up for next test Approx. Moves: _____
- ☐ Phase 3 300/550/900 Wrist/Reach
- ☐ 3 min Break and Set up for next test Approx. Moves: _____
- ☐ Phase 4 300/550/900 Wrist/Reach
- ☐ 3 min Break and Set up for next test Approx. Moves: _____
- ☐ Phase 5 300/550/900 Wrist/Reach
- ☐ 3 min Break and Set up for next test Approx. Moves: _____
- ☐ Phase 6 300/550/900 Wrist/Reach
- ☐ Finish Time: _____ Approx. Moves: _____
- ☐ Ask if there are any comments:

_____

_____

_____

- ☐ Ask if there are any questions:

_____

_____

_____

## APPENDIX C: INSTRUCTIONAL POWERPOINT

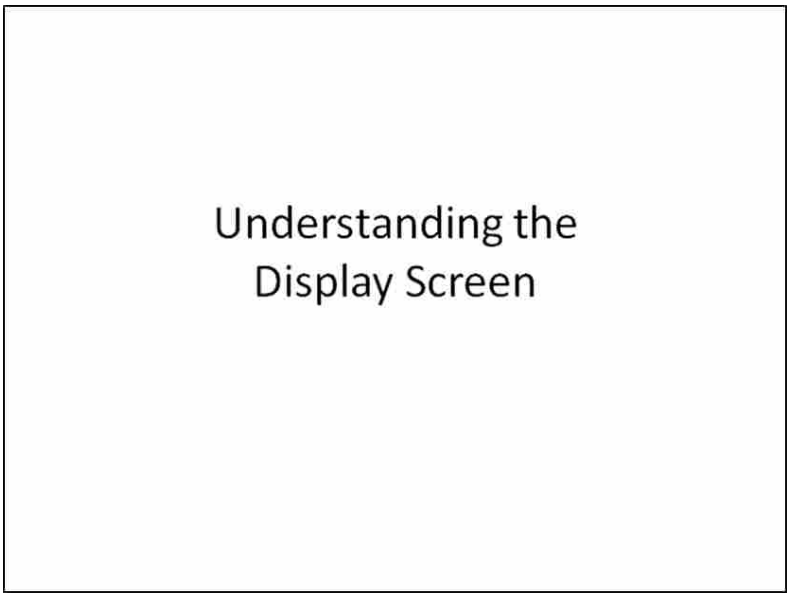


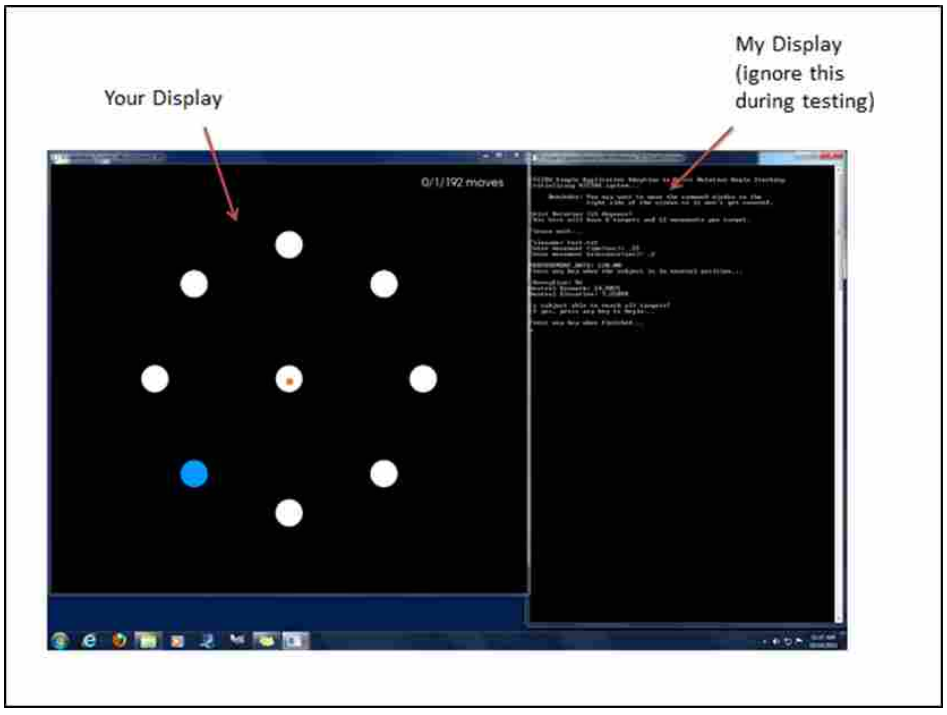

Your cursor (orange) will start in the center, and targets (blue) will light up for you to hit.

Once you leave a circle, you have a certain amount of time to get to the next target. Each move should be one *continuous* and *straight* movement.

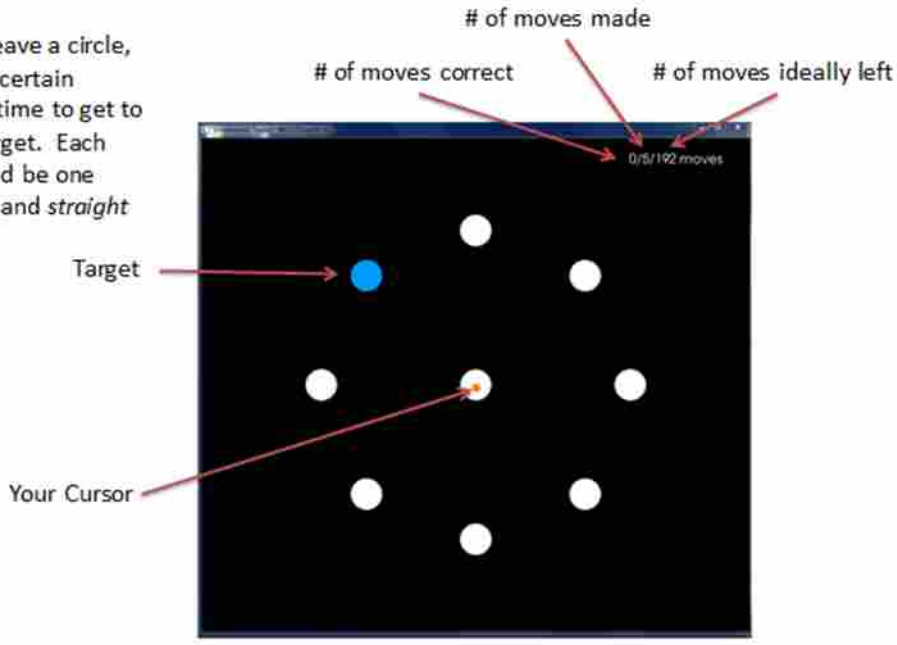


If you go too slow (.x sec slower than the certain amount of time), you will be given a green circle with a prompt on the top right to "Go Faster"

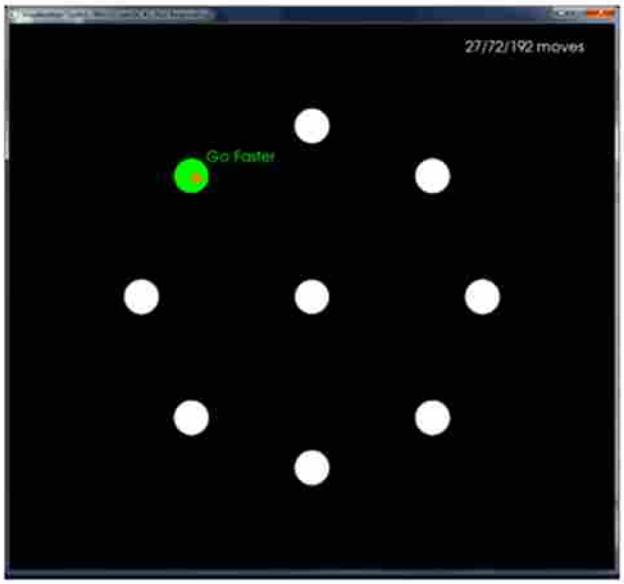

If you go too fast (.x sec faster than the certain amount of time), you will be given a red circle with a prompt on the top right to "Go Slower"

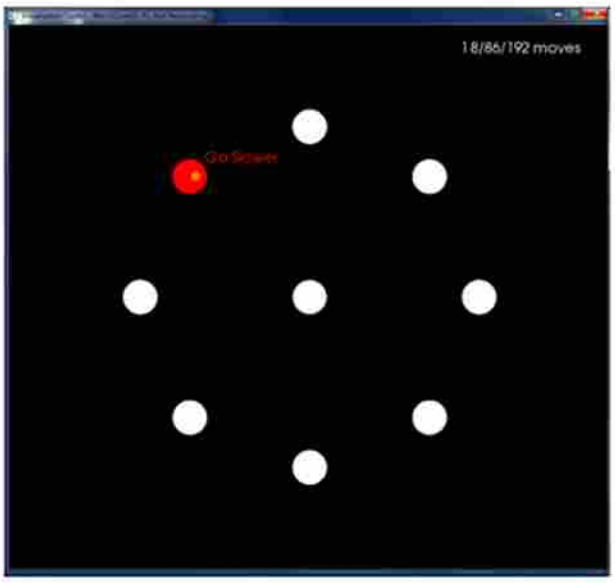


If you reach the target at a good speed (within .x sec of the certain amount of time), the circle will remain white with a prompt on the top right "Good Job!"

Correct moves will only begin to count after 32 practice moves

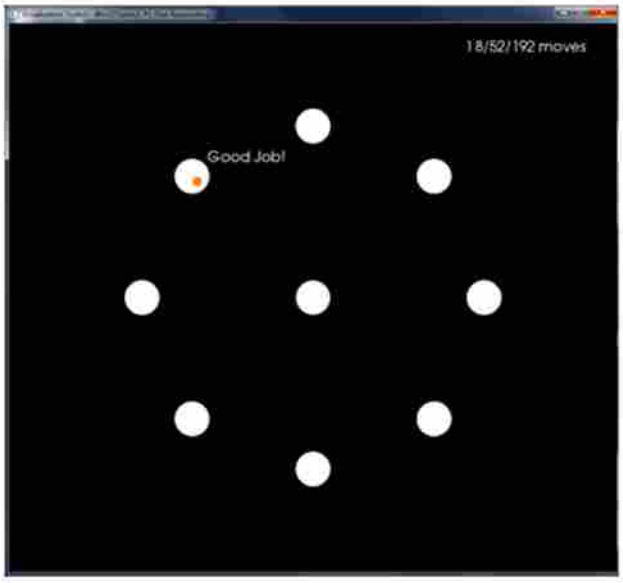

After you have stayed within the circle for .6 sec, you will then be prompted to return to the center, which will light up as a target. These moves will also be timed, just like the outward moves

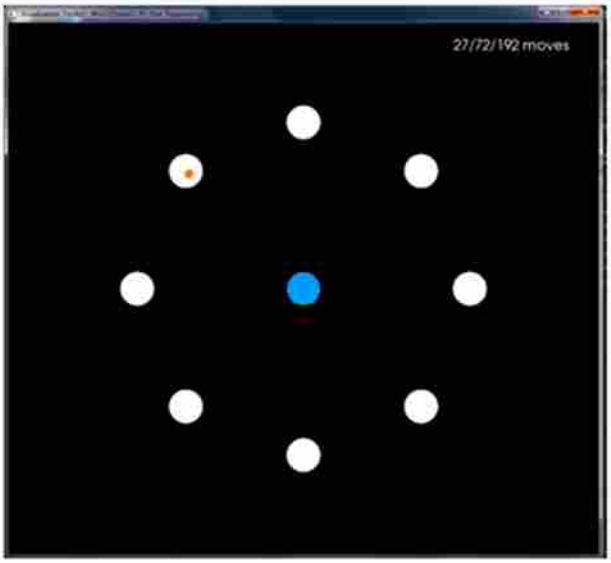


1) When exactly does the timer start and end? Leaves and enters the circles
2) How many *correct* moves do you need to do to finish a run? At least 160
3) How many total moves are there per run? Indefinite, depends on performance

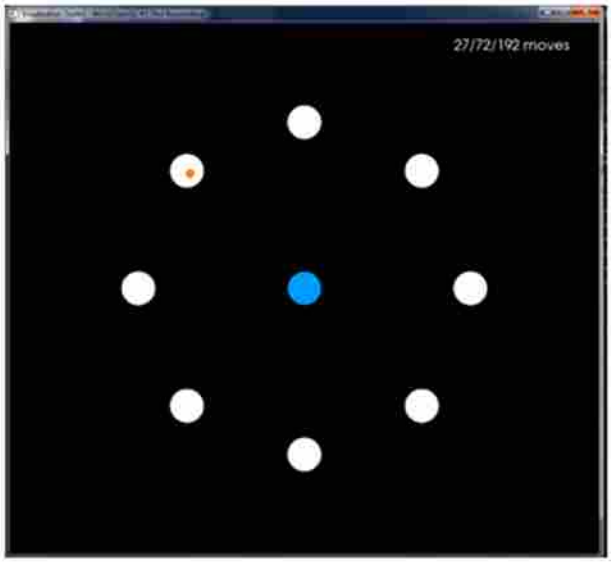

## APPENDIX D: EFFECTS OF FILTER CUT-OFF FREQUENCY AND ORDER

The following plots and tables detail the effects of varying filtering properties on cut-off frequency and the order of the Butterworth filter. These plots are discussed in Section 3.7 and Section 4.2. The sequence of different filtering properties is as follows:

1. 5Hz cut-off frequency with $6^{th}$ order Butterworth filter
2. 10Hz cut-off frequency with $6^{th}$ order Butterworth filter
3. 20Hz cut-off frequency with $6^{th}$ order Butterworth filter
4. 25Hz cut-off frequency with $6^{th}$ order Butterworth filter
5. 15Hz cut-off frequency with $2^{nd}$ order Butterworth filter

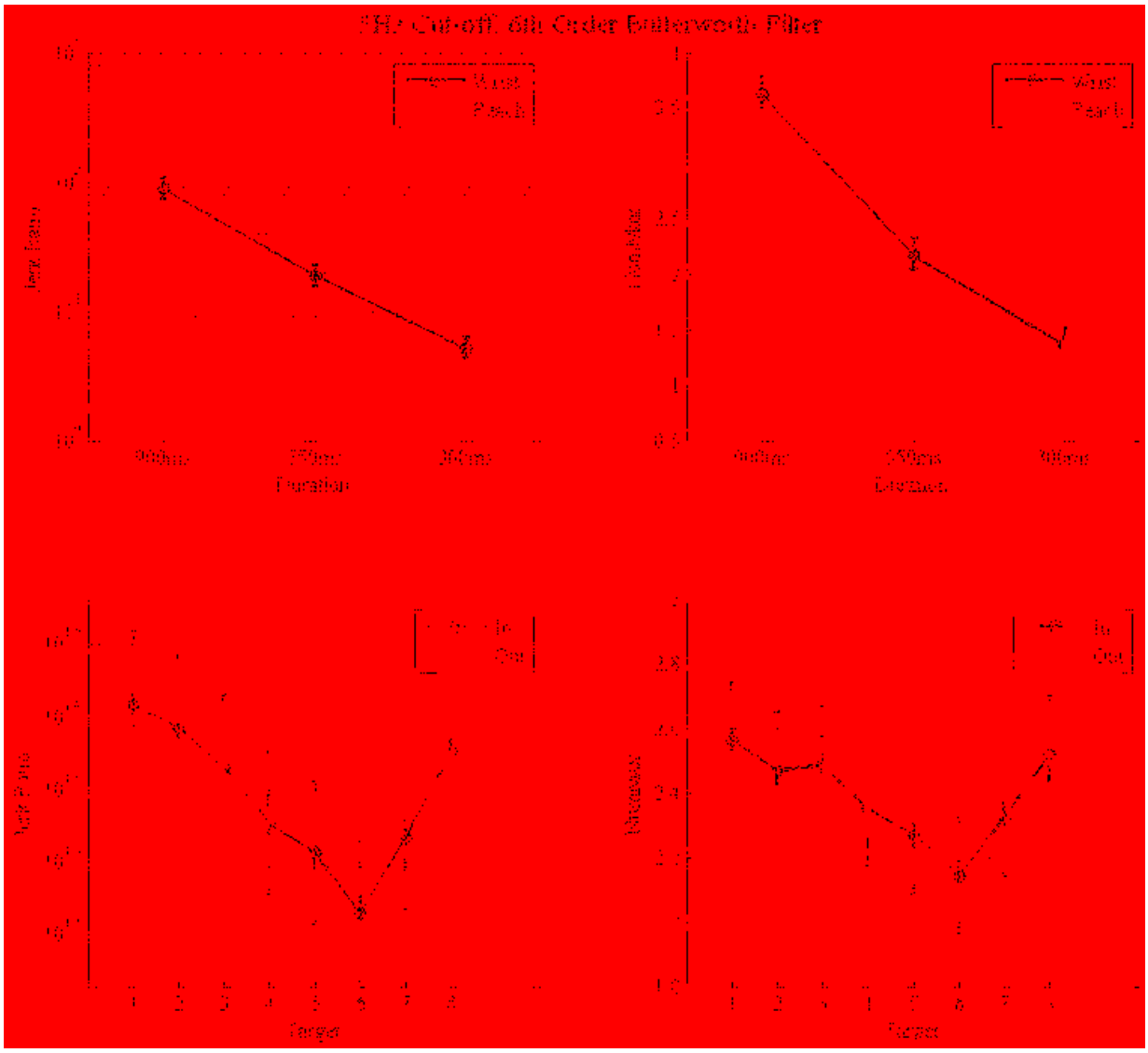

| Measure | Data | Effect | Num DF | Den DF | F Value | Pr > F |
|---|---|---|---|---|---|---|
| logJerkRatio | Reach/Wrist | Joint | 1 | 9 | 311.41 | <.0001 |
| logJerkRatio | Wrist only | Speed | 2 | 18 | 398.08 | <.0001 |
| logJerkRatio | Wrist only | Target | 7 | 63 | 0.59 | 0.7637 |
| logJerkRatio | Wrist only | Direction | 1 | 9 | 7.19 | 0.0251 |
| logJerkRatio | Reach/Wrist | Joint*Speed | 2 | 18 | 26.99 | <.0001 |
| logJerkRatio | Wrist only | Target*Direction | 7 | 63 | 21.21 | <.0001 |
| NumMax | Reach/Wrist | Joint | 1 | 9 | 261.81 | <.0001 |
| NumMax | Wrist only | Speed | 2 | 18 | 571.48 | <.0001 |
| NumMax | Wrist only | Target | 7 | 63 | 0.61 | 0.7447 |
| NumMax | Wrist only | Direction | 1 | 9 | 0.13 | 0.7234 |
| NumMax | Reach/Wrist | Joint*Speed | 2 | 18 | 125.96 | <.0001 |
| NumMax | Wrist only | Target*Direction | 7 | 63 | 17.23 | <.0001 |

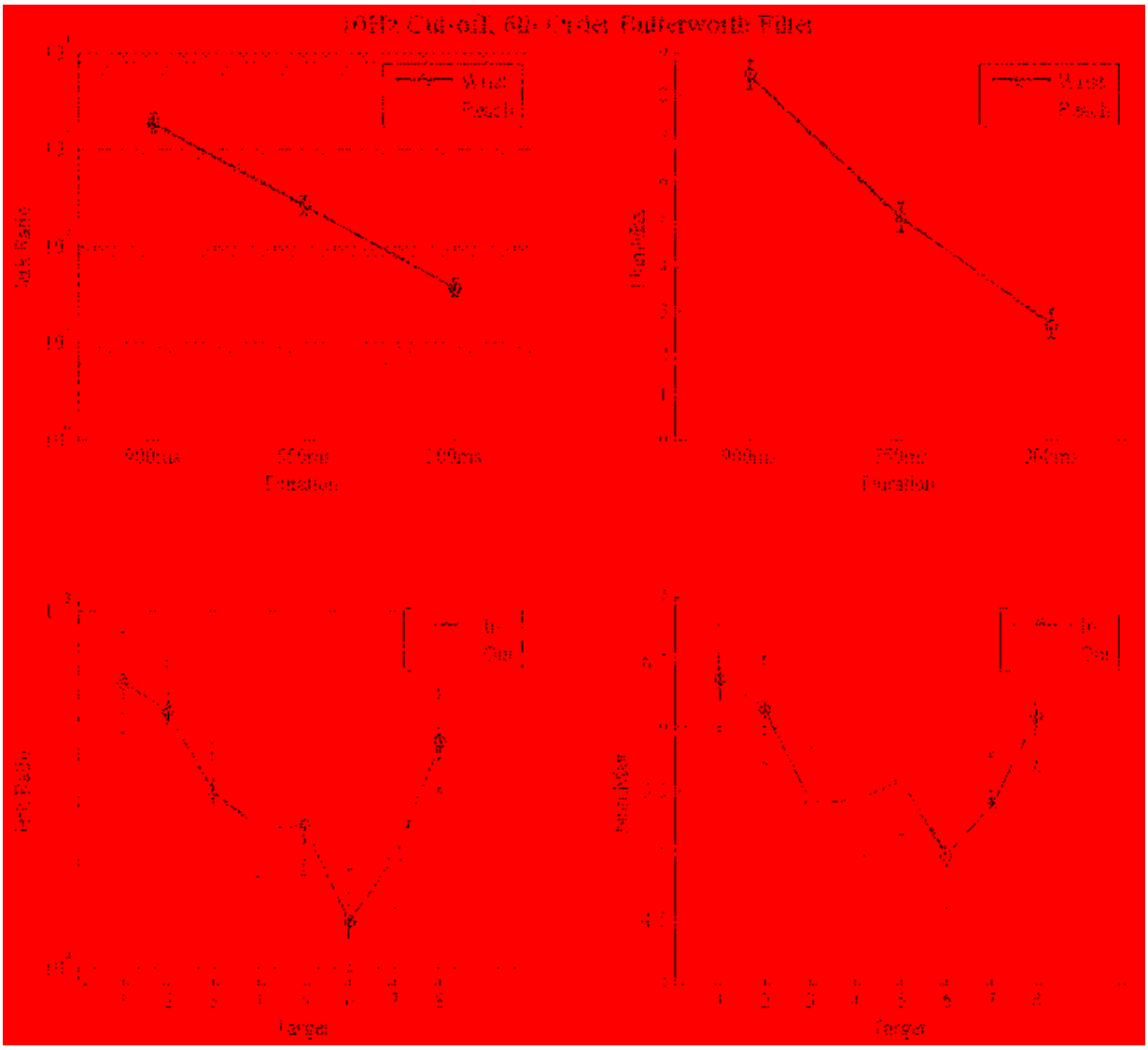

| Measure | Data | Effect | Num DF | Den DF | F Value | Pr > F |
|---|---|---|---|---|---|---|
| logJerkRatio | Reach/Wrist | Joint | 1 | 9 | 517.61 | <.0001 |
| logJerkRatio | Wrist only | Speed | 2 | 18 | 1420.83 | <.0001 |
| logJerkRatio | Wrist only | Target | 7 | 63 | 3.29 | 0.0048 |
| logJerkRatio | Wrist only | Direction | 1 | 9 | 26.29 | 0.0006 |
| logJerkRatio | Reach/Wrist | Joint*Speed | 2 | 18 | 15.65 | 0.0001 |
| logJerkRatio | Wrist only | Target*Direction | 7 | 63 | 35.71 | <.0001 |
| NumMax | Reach/Wrist | Joint | 1 | 9 | 277.46 | <.0001 |
| NumMax | Wrist only | Speed | 2 | 18 | 523.24 | <.0001 |
| NumMax | Wrist only | Target | 7 | 63 | 5.91 | 0.0001 |
| NumMax | Wrist only | Direction | 1 | 9 | 41.81 | <.0001 |
| NumMax | Reach/Wrist | Joint*Speed | 2 | 18 | 62.1 | <.0001 |
| NumMax | Wrist only | Target*Direction | 7 | 63 | 11.98 | <.0001 |

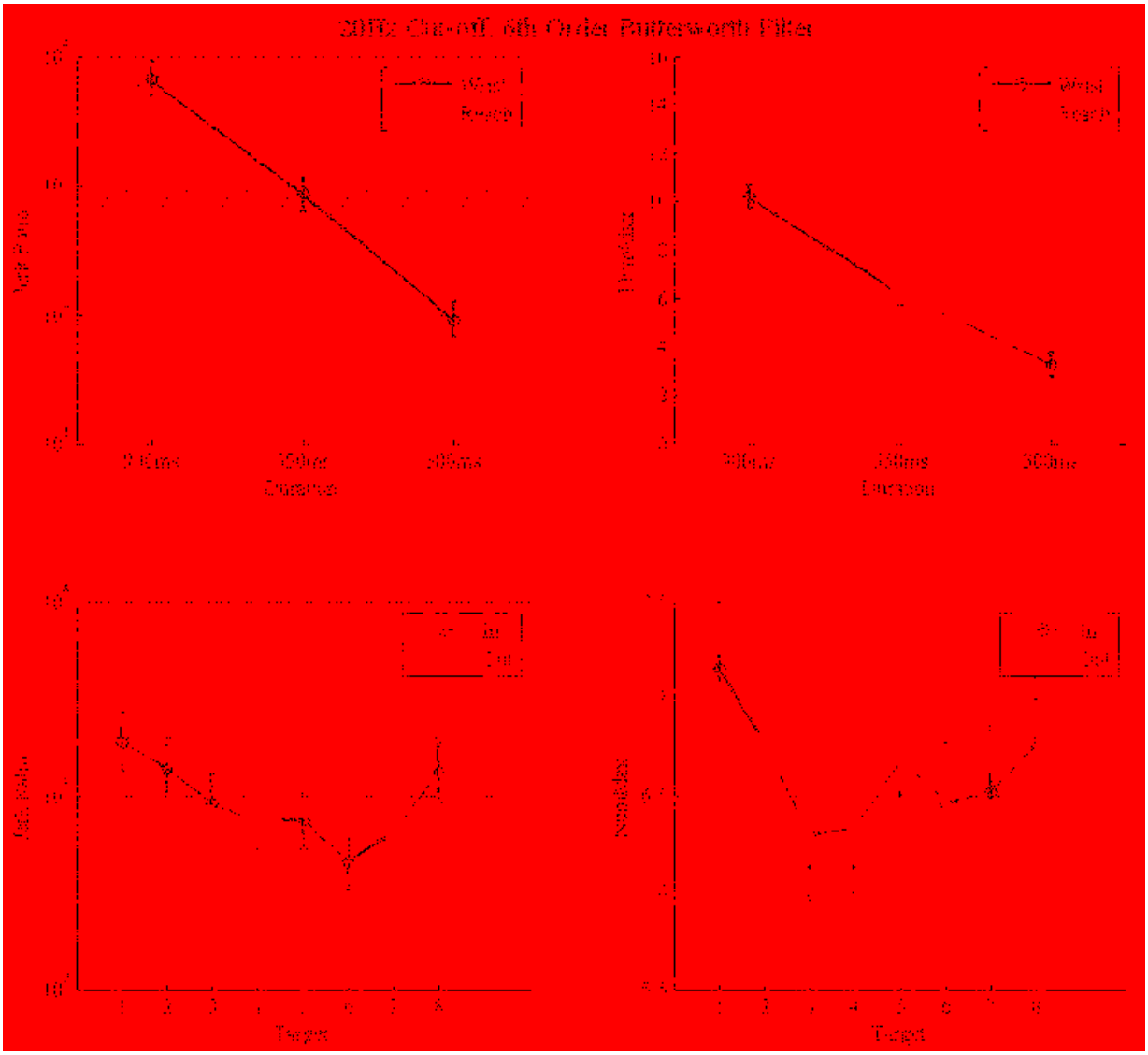

| Measure | Data | Effect | Num DF | Den DF | F Value | Pr > F |
|---|---|---|---|---|---|---|
| logJerkRatio | Reach/Wrist | Joint | 1 | 9 | 43.14 | 0.0001 |
| logJerkRatio | Wrist only | Speed | 2 | 18 | 798.88 | <.0001 |
| logJerkRatio | Wrist only | Target | 7 | 63 | 5.62 | <.0001 |
| logJerkRatio | Wrist only | Direction | 1 | 9 | 27.3 | 0.0005 |
| logJerkRatio | Reach/Wrist | Joint*Speed | 2 | 18 | 18.73 | <.0001 |
| logJerkRatio | Wrist only | Target*Direction | 7 | 63 | 26.72 | <.0001 |
| NumMax | Reach/Wrist | Joint | 1 | 9 | 22.41 | 0.0011 |
| NumMax | Wrist only | Speed | 2 | 18 | 566.97 | <.0001 |
| NumMax | Wrist only | Target | 7 | 63 | 4.57 | 0.0004 |
| NumMax | Wrist only | Direction | 1 | 9 | 4.12 | 0.0728 |
| NumMax | Reach/Wrist | Joint*Speed | 2 | 18 | 122.38 | <.0001 |
| NumMax | Wrist only | Target*Direction | 7 | 63 | 3.56 | <.0001 |

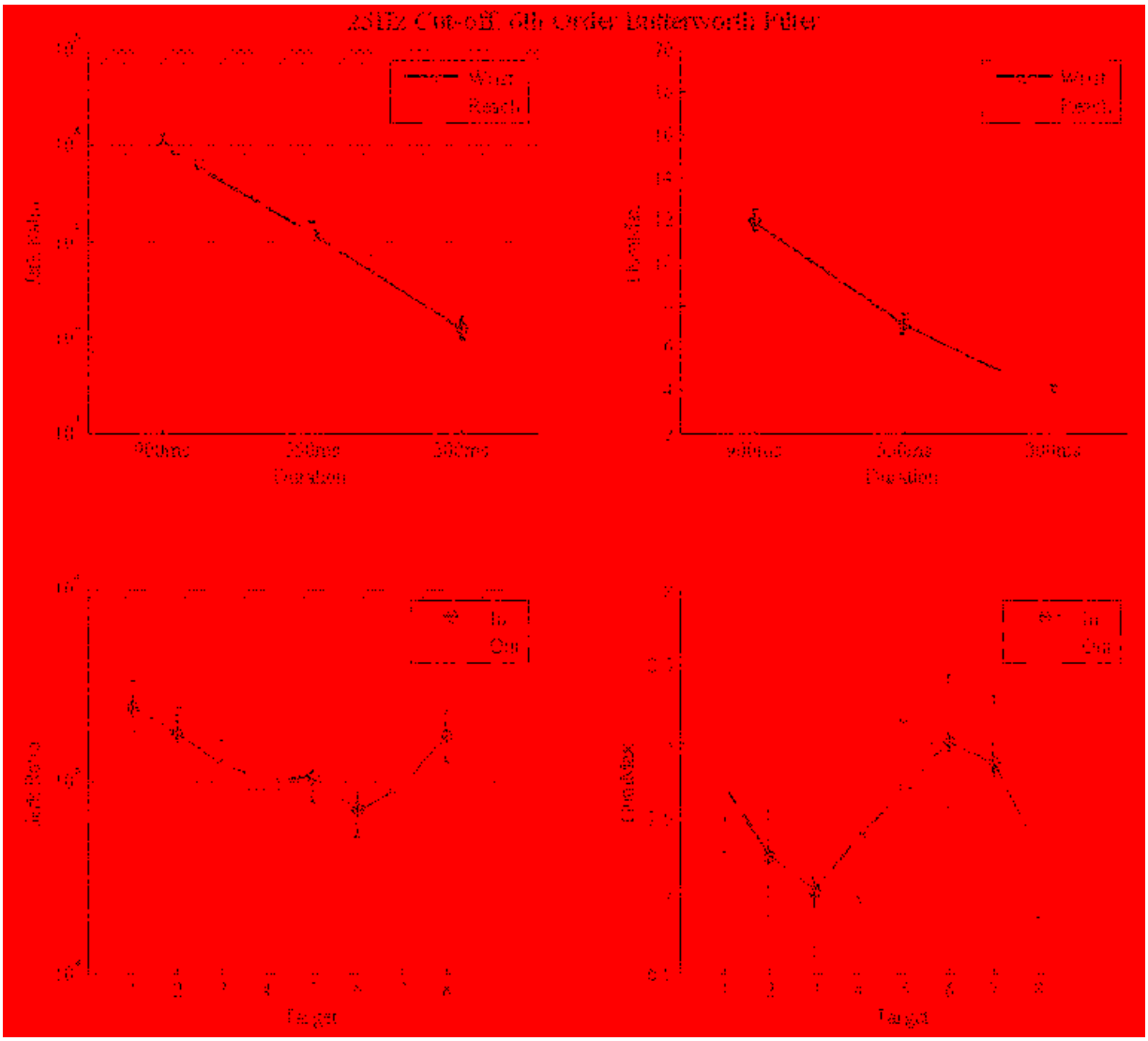

| Measure | Data | Effect | Num DF | Den DF | F Value | Pr > F |
|---|---|---|---|---|---|---|
| logJerkRatio | Reach/Wrist | Joint | 1 | 9 | 15.61 | 0.0034 |
| logJerkRatio | Wrist only | Speed | 2 | 18 | 965.8 | <.0001 |
| logJerkRatio | Wrist only | Target | 7 | 63 | 4.44 | 0.0005 |
| logJerkRatio | Wrist only | Direction | 1 | 9 | 19.24 | 0.0018 |
| logJerkRatio | Reach/Wrist | Joint*Speed | 2 | 18 | 16.98 | <.0001 |
| logJerkRatio | Wrist only | Target*Direction | 7 | 63 | 21.28 | <.0001 |
| NumMax | Reach/Wrist | Joint | 1 | 9 | 205.81 | <.0001 |
| NumMax | Wrist only | Speed | 2 | 18 | 464.07 | <.0001 |
| NumMax | Wrist only | Target | 7 | 63 | 1.5 | 0.1831 |
| NumMax | Wrist only | Direction | 1 | 9 | 0.36 | 0.5623 |
| NumMax | Reach/Wrist | Joint*Speed | 2 | 18 | 202.36 | <.0001 |
| NumMax | Wrist only | Target*Direction | 7 | 63 | 5.37 | <.0001 |

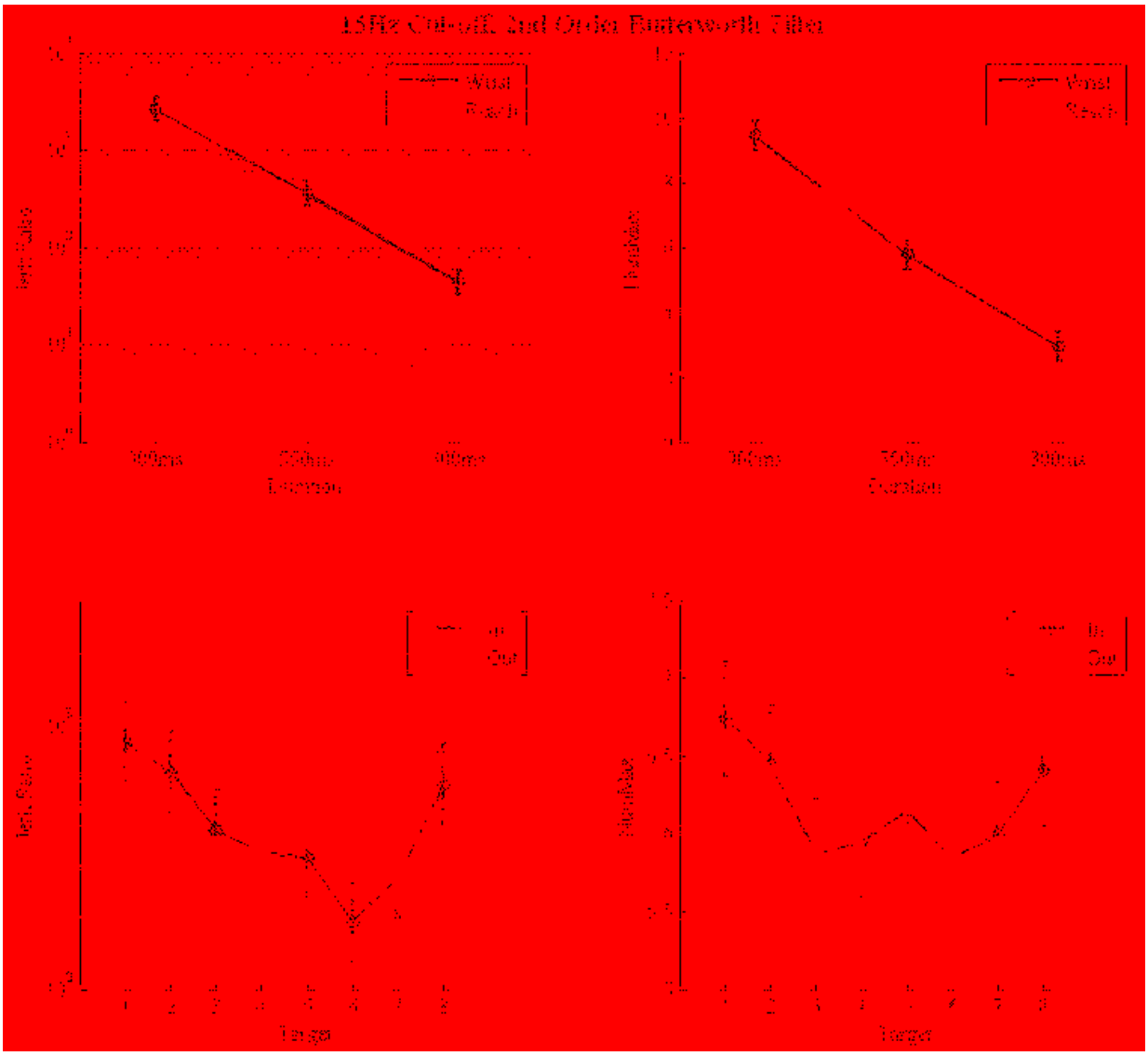

| Measure | Data | Effect | Num DF | Den DF | F Value | Pr > F |
|---|---|---|---|---|---|---|
| logJerkRatio | Reach/Wrist | Joint | 1 | 9 | 202.52 | <.0001 |
| logJerkRatio | Wrist only | Speed | 2 | 18 | 870.82 | <.0001 |
| logJerkRatio | Wrist only | Target | 7 | 63 | 4.71 | 0.0003 |
| logJerkRatio | Wrist only | Direction | 1 | 9 | 33.33 | 0.0003 |
| logJerkRatio | Reach/Wrist | Joint*Speed | 2 | 18 | 1.25 | 0.3114 |
| logJerkRatio | Wrist only | Target*Direction | 7 | 63 | 37.1 | <.0001 |
| NumMax | Reach/Wrist | Joint | 1 | 9 | 4.71 | 0.0582 |
| NumMax | Wrist only | Speed | 2 | 18 | 592.09 | <.0001 |
| NumMax | Wrist only | Target | 7 | 63 | 5.61 | <.0001 |
| NumMax | Wrist only | Direction | 1 | 9 | 16.53 | 0.0028 |
| NumMax | Reach/Wrist | Joint*Speed | 2 | 18 | 47.57 | <.0001 |
| NumMax | Wrist only | Target*Direction | 7 | 63 | 6.49 | <.0001 |

## APPENDIX E: LITERATURE REVIEW ON REACHING PARAMETERS CHART

This literature review was meant to gather the stiffness, damping, inertia, and other mechanical properties of the arm and determine the method of how the properties were obtained. The purpose was to find the most reliable values, and the properties that would most closely follow the experiment that was performed in this research.

The literature review include many studies (Lacquaniti et al., 1982; Mussa-Ivaldi et al., 1985; MacKay et al., 1986; Flash and Mussa-Ivaldi, 1990; Bennett et al., 1992; Bennett, 1993; Milner, 1993; Shadmehr and Mussa-Ivaldi, 1994; Tsuji et al., 1994, 1995, 2004; Gomi and Kawato, 1997; Gomi and Osu, 1998; Stroeve, 1999; Burdet et al., 2000, 2013; Tee et al., 2004, 2010; Franklin et al., 2004, 2007; Selen et al., 2009). For the arm, all parameters were taken from Tee et al. (2004) and solved for using the methods described in Tee et al. (2004) because the methods modeled reaching movement well and we decided to use the same methods. Therefore, we also used the values from Tee et al. (2004), although some of the values used in Tee et al. (2004) were from other previous studies.

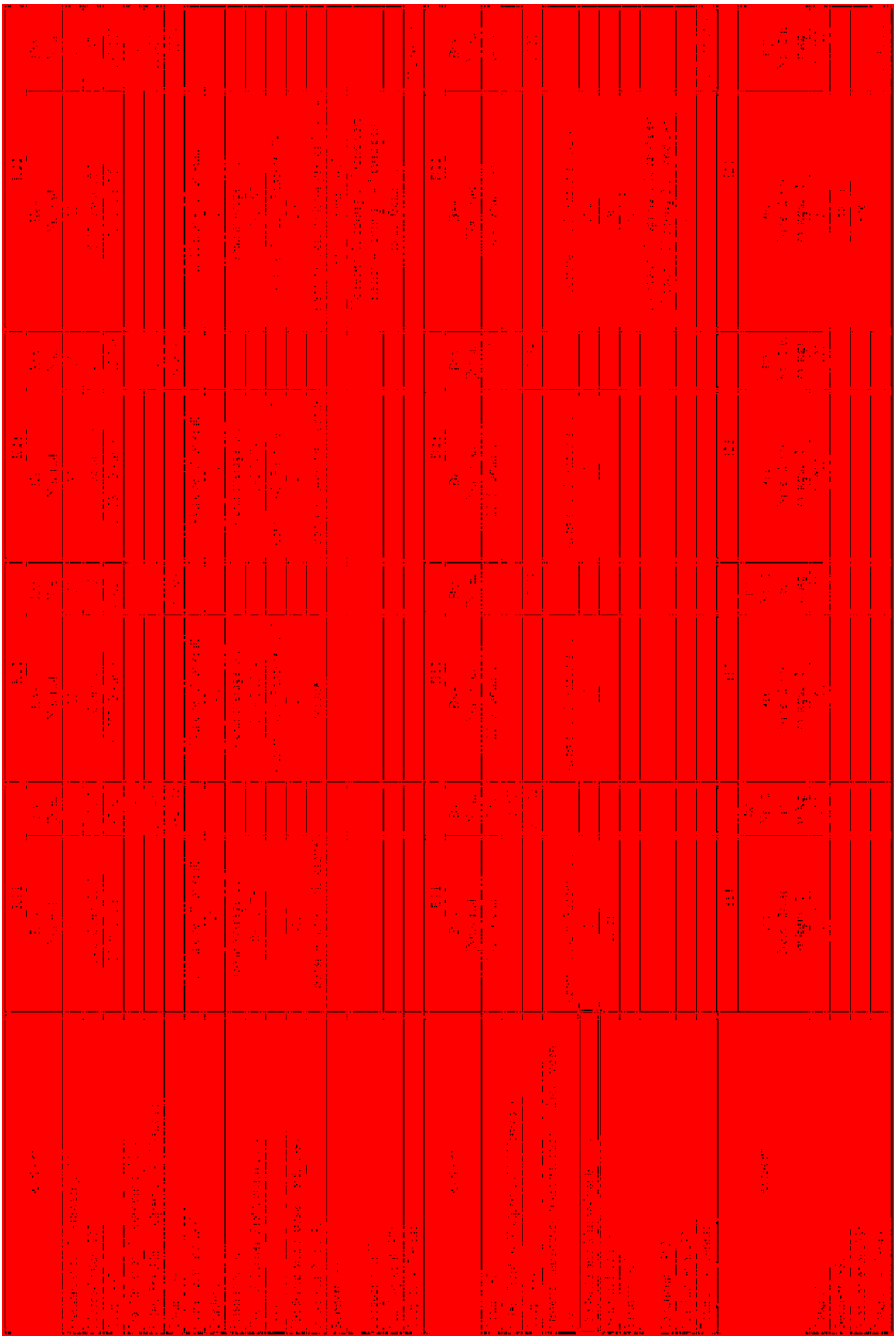

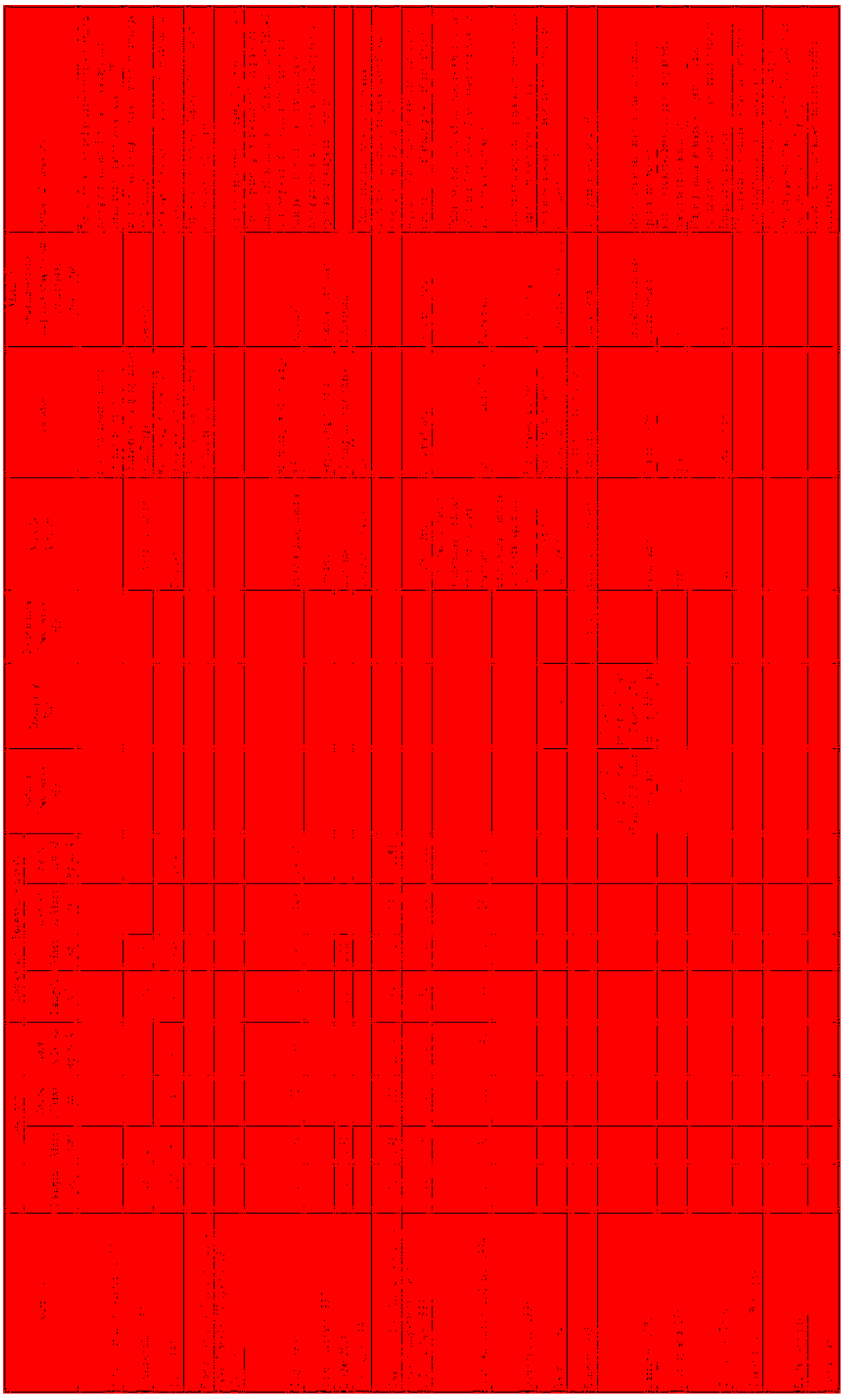

## APPENDIX F: REDUCTION OF NUMERICAL ERROR IN SIMULATION

This table was used to reduce the numerical error in the simulation of Hypothesis 1-2. The first column details the variables that were left constant for the trial, the second column contained the variable that was altered, and the next 3 columns contained the 3 durations Jerk Ratio (JR) mean and standard deviation. The last column contains comments of the tests. The top chart is for reference to the actual values of Jerk Ratio, which was used to compare to the model with filtering and noise that is bolded on the bottom chart. The bold rows were the chosen variables for the model.